Residual Stress Calculations and Measurements - Review and Assessment of the IIW Round Robin Results

Helmut Wohlfahrt [*], Thomas Nitschke-Pagel [*], Klaus Dilger [*], Dieter Siegele [**], Marcus Brand [**], Jens Sakkiettibutra [***], and Tobias Loose[****]

[*] Institute of Joining and Welding, University of Braunschweig, Germany,
[**] Fraunhofer-Institut for Mechanics of Materials, Freiburg, Germany,
[***] Bremer Institut für angewandte Strahltechnik GmbH, Bremen,
[****] Ingenieurbüro Tobias Loose GbR, Karlsruhe

Abstract

A Round Robin Programme was established by a working group of Commission X in 1997 in order to evaluate the possibilities of residual stress and distortion prediction (RSDP) in welded structures and to validate and benchmark prediction codes based on finite element simulation of the welding process. Calculations on residual tresses have been carried out of an austenitic steel plate with well defined material and geometrical data, welding conditions and with the proposal to use the kinematic hardening model.

In addition a second programme for measurements of residual stresses in this plate has been started in 2003. Measurements have been taken on three austenitic steel plates using the X-ray measuring method as well as neutron diffraction methods and different kinds and variations of the hole drilling method.

Although a rough agreement between the measured results and the calculated ones was found in principle, distinct differences have been observed in detail – especially for the longitudinal residual stresses. The calculations indicated nearly constant tensile stresses of the order of the initial yield strength in the weld seam and in the adjacent heat affected zone (HAZ). The measurements however revealed stress maxima in the HAZ with values clearly higher than the initial yield strength. Therefore additional calculations have been carried out with different hardening models in order to investigate their influence on the residual stress results. In fact, calculations performed with the isotropic hardening model could approve these stress maxima quite exactly.

In further detailed investigations it could be shown that the reason for the stress maxima is the strain hardening in the HAZ due to thermal stresses during the welding process. Finally basic considerations could explain that the kinematic hardening model, including the Bauschinger effect, cannot account for this hardening effect. Literature indicates that the Bauschinger effect is at least not fully effective at high working temperatures of austenitic steels. Altogether, the calculation programme has shown that a rather rough estimation of the residual stress state after welding is possible without any special distinction of the hardening model to be used. For a more precise and detailed information the chosen hardening model is of significant relevance.

Keywords

Welding simulation, numerical simulation, residual stresses, welding distortions, strain hardening, X-ray diffraction, neutron diffraction, hole drilling measurements, austenitic steel.

1. Intention of the Round Robin Programme

A Round Robin Programme was established by a working group of Commission X in 1997 in order to evaluate the possibilities of Residual Stress and Distortion Prediction (RSDP) in welded structures and to validate and benchmark prediction codes based on finite element simulation of the welding process. In addition to the calculation programme (RSDP phase I and phase II) on residual stresses in an austenitic steel plate a second programme for measurements of residual stresses in this plate has been started in 2003. The intention was to compare the results of both programmes and thus to validate both methods alternately.

However, significant differences have been found between the calculations of longitudinal residual stresses according to the RSDP programme, phase II, and the measured longitudinal residual stresses. Therefore, additional calculations seemed to be necessary in order to investigate the influence of the material model used in the simulation of the welding process on the calculated residual stresses. Whereas in the RSDP programme a kinematic material law was recommended additional calculations have been carried out with the material laws of isotropic hardening, kinematic hardening, mixed hardening and ideal elastic-plastic material behaviour.

2. Basic Items of the Round Robin Programme

2.1 Welded Austenitic Steel Plate

As a reference for calculations and as a test object for measurements three plates of the low-carbon austenitic stainless steel 316LNSPH (dimensions in **Fig. 1**) have been used. Each plate was supported at three points. In a prefabricated U-shaped groove (depth approx 7 mm) along the 270 mm long middle line two passes of filler material (316L, 1.2 mm diameter) have been deposited with tungsten inert gas welding (GTAW). The thermal cycles during welding of both deposits have been controlled by four thermocouples on the upper surface of the plate at different positions along the seam and in different distances from the fusion line. The measured thermal cycles during welding in a laboratory of the Electricité de France Company are registered in [1], where also more details about the welding conditions and a database of the thermal and mechanical material properties are given. **Fig. 2** illustrates the macrographs of the first and second pass of the weld seam.
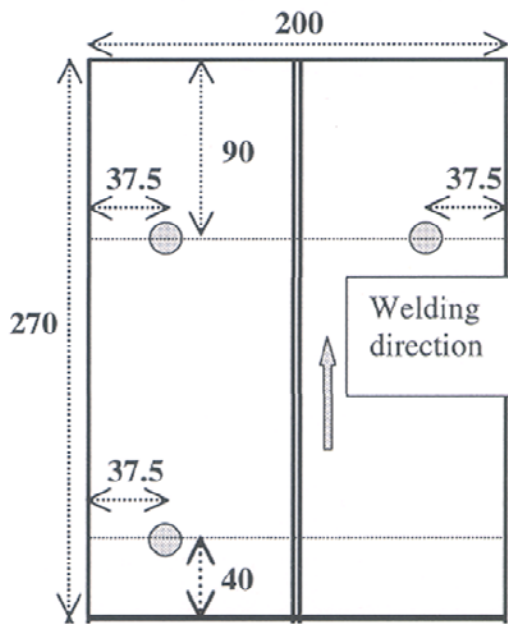
Fig. 1 Geometry of the plate, dimensions in mm, plate thickness: 30 mm [1]
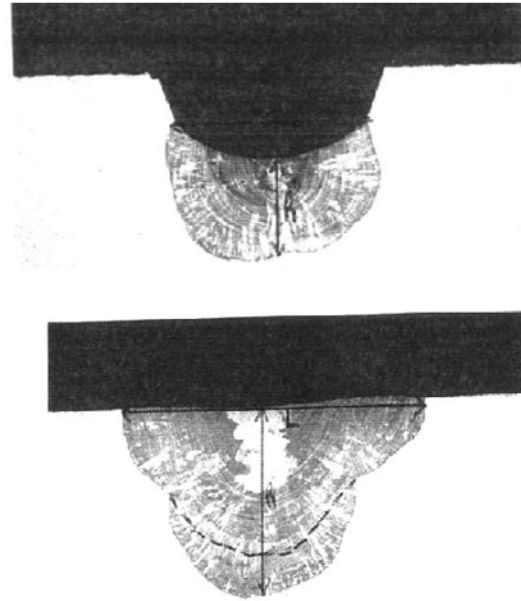

Fig. 2 Macrographs of the 1st pass (h = 2.7 mm, 17.5 mm^2) and 2nd pass (h = 5.9 mm, total welded zone 38.5 mm^2) [1]

2.2 Conditions and requirements of calculations

2.2.1 CONDITIONS AND REQUIREMENTS OF RSDP (PHASE I and) PHASE II

For modelling of the heat input from the welding process the finite element programme SYSWELD was mainly used and for modelling the materials deformation behaviour the kinematic hardening model was recommended. For comparison of the results from the different participants it was proposed to calculate the longitudinal, transverse and radial residual stresses versus the thickness of the plate (line 1 and line 2 in **Fig. 3**) and along lines transverse to the seam at the top side and the bottom side of the plate (line 3 and line 4).
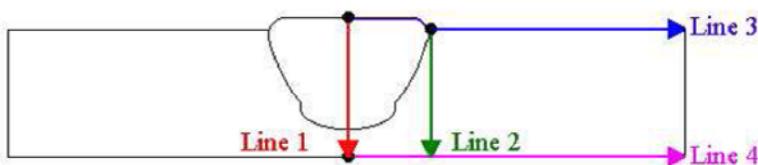

Fig. 3 Lines along which stress calculations have been requested

The RSDP benchmark has been started in phase I with 2D analyses but the numerical results turned out to need a significant improvement of the quality. As main influence factors on the results the modelling of the heat input, the mesh size near the notch, the assumption of the stress state in the third direction (plane stress, plane strain) and the strain history were identified [2]. Therefore, a second part of the Round Robin has been started with 3D modelling of the geometry and the moving of the heat source. As a first important validation of the modelling of the temperature distribution the thermal cycles have been compared with the temperature cycles measured during the welding process. Here, the peak temperature and the slope of the temperature profile were identified as the main critical factors influencing the results [3].

2.2.2 CONDITIONS AND REQUIREMENTS OF ADDITIONAL CALCULATIONS

The additional 3D thermo-mechanical simulations have been performed in 2008 with the finite element programme SYSWELD (version 2008.1). The plate has been discretised by 55.000 linear volume elements of the type "3008". The elements representing the weld pool have an edge-length of 1 mm. **Fig. 4** shows the surface and a cross-section of the finite element mesh. To simulate the material input of the filler material during welding, the elements representing the filler material were modelled to have an artificial reduced Young's modulus of 1.000 MPa before welding and if the elements are heated over 1450 °C (melting temperature) during welding the material state was changed to real material properties. Considering the melting of the material, the accumulated plastic strains and the hardening were reset (command "TF") when the melting temperature was achieved. Isotropic, kinematic and mixed hardening models were selected.
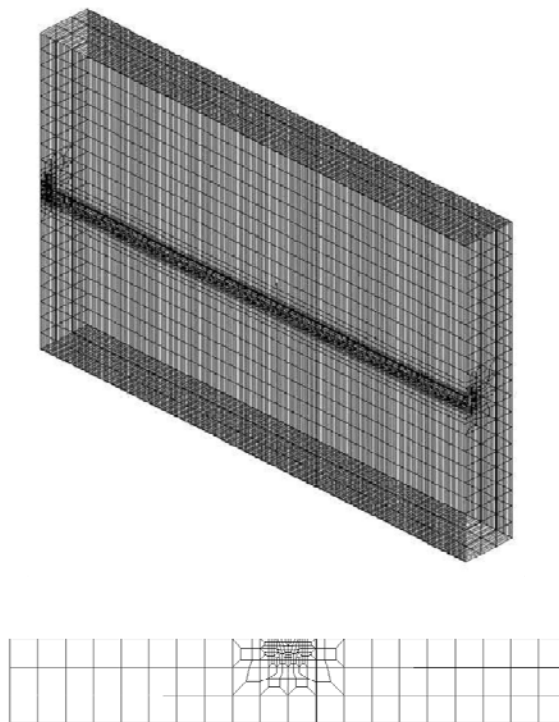

Fig. 4 The surface and a cross section of the mesh

The thermo-mechanical calculation was performed in two sequentially calculated steps. At first, the temperature distributions, known as the heat effect of welding [4], were calculated. A comparison of measured thermocycles and calculated temperature-time curves in different distances from the weld pool is given in **Fig. 5**. Afterwards, the resulting mechanical behaviour is calculated with the calculated temperature distribution as a main input. In different analyses, the heat input was modelled using the Goldak heat source [6] or other heat sources like a conical heat source as used for temperature-field calculation as shown in **Fig. 5**. Geometrical parameters of the heat sources have been fitted to the measured thermocycles. More details about the conditions of these calculations can be found in [7]. For the given thermophysical properties of austenitic material an excellent agreement between measurement and simulation of the temperature distribution can be achieved.
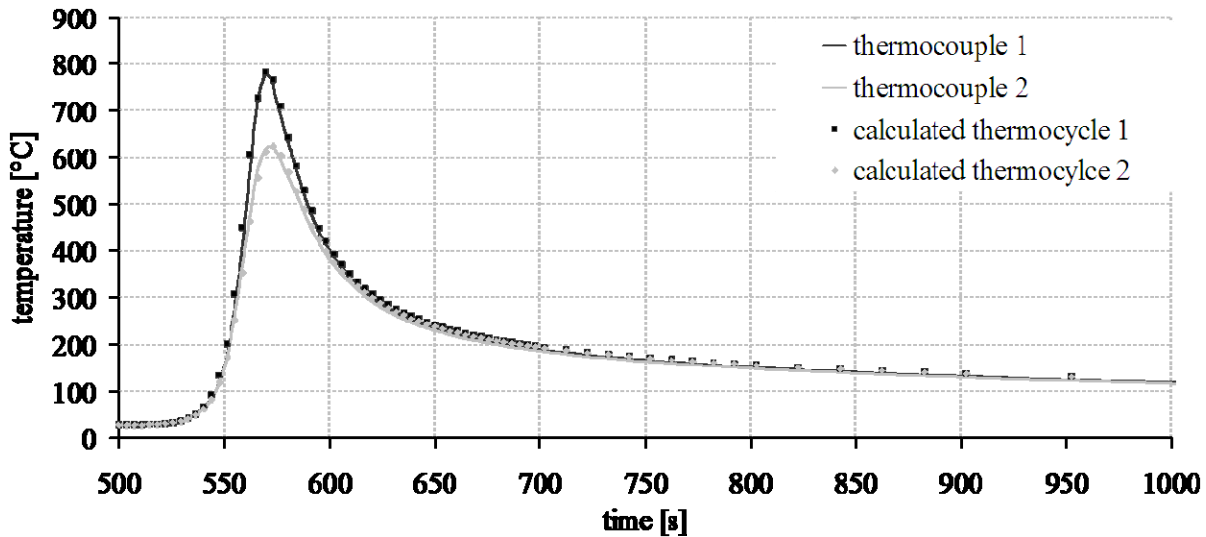
Fig. 5 Comparison of measured and calculated thermocyles across to the weld for the 1st pass using a conical heat source [5]

2.3 Conditions and requirements of measurements

The intention of the measurement programme was the determination of the residual stresses at the surface and also in deeper layers by means of different non-destructive and semi-destructive methods using the possibilities of various laboratories. The longitudinal and transverse residual stress components should be measured at different distances from the weld centre line along the line 3 in **Fig. 3** with non-destructive techniques and along lines parallel to the line 3 in appropriate distances from each other with semi-destructive hole drilling techniques according to **Fig. 6**, respectively. With neutron diffraction it was also possible to measure the residual stresses along a line parallel to the line 3 in deeper layers. Depth profiles of the longitudinal and the transverse residual stresses have been taken along line 1 (**Fig. 3**) with neutron diffraction and with the deep hole drilling method and also parallel to line 1 in a distance of about 7 mm from the weld centre line with neutron diffraction. Additionally, it seemed interesting to measure both residual stress components along a line perpendicular to the seam on the backside of the plate (line 4).
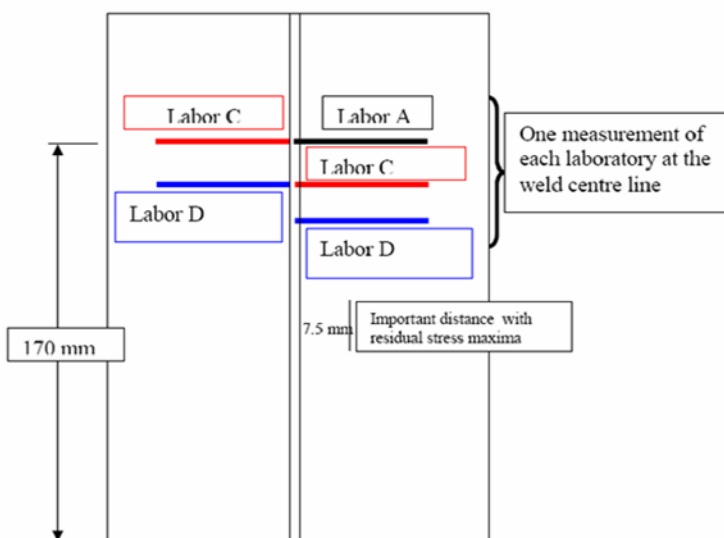

Fig. 6 Plan for measurements of different laboratories with the X-ray and with the hole drilling method [8]

The participants of the measuring programme, their various measuring methods and important parameters of the different techniques are summarized in **Table 1** and **Table 2**.

Table 1 Institutions using the non-destructive measuring techniques X-ray diffractometry or neutron diffraction. Reflecting lattice planes γ-Fe {311}, E = 196 GPa, ν = 0.28 (X-ray) or ν = 0.3 (neutron diffraction). Order of the institutions according to the date of measurements.

Measurements with X-ray diffractometry				
Institution	Measuring positions	Measuring method, radiation	Detector, spot size, irradiated area	Ψ-tilt angles
Institut für Füge- und Schweißtechnik, University of Braunschweig, Dr. Nitschke-Pagel	on a line transverse to the seam, ca. 200 mm from beginning of the seam, only transverse stresses	X-ray diffractometer, $\sin^2\Psi$-method, Cr-radiation		
Fraunhofer-Institut Werkstoffmechanik, Freiburg, Germany, Dr. Pfeiffer	on a line transverse to the seam, 170 mm from begin-ning of the seam	X-ray STRESSTECH X3000, $\sin^2\Psi$-method, Mn Kα–radiation	2 mm diameter 2x22 mm^2, oscillation	11 between +/-45^0
CETIM, Senlis, France, Dr. Lieurade	on a line transverse to the seam, 110 mm from beginning of the seam	X-ray portable unit, multiple linear re-gression, Mn Kα-radiation	position sensitive spot size 2.5 mm diameter	7 between $0<\sin^2\Psi<0.5$
Czech Techn. University Prague, Czech Republic, Dr. Ganev	on a line transverse to the seam, 50 mm from beginning of the seam	portable diffractometer, system. for analysis LUCIA, Cr Kβ–radiation	position sensitive spot size 2 mm, 2x22 mm^2, oscillation	
Hitachi Res. Laboratory, Japan, Dr, Shinobu Okido	on five lines transverse to the seam, app.. 20 mm to 66 mm from begin-ning of the seam	X-ray diffractometer, $\sin^2\Psi$ method, fit with elliptical function, Mn Kα–radiation	position sensitive spot size 2 and 3 mm, oscillation	11 between +/-41.6^0

Measurements with neutron diffraction			
Institution	Measuring positions, depth, distance from the beginning of the seam	Measuring method, wavelength, diffraction angle	Gauge volume
GKSS Res. Laboratory, Geesthacht, Germany Dr. Staron	on lines transverse to the seam, depth 3mm and 15 mm; 170 mm from beginning of the seam; in-depth scan: along line 1, Fig.3	Neutron diffractometer ARES, 0.1647 mm, 98.4^0	longitud. 3x3x3 mm^3, transverse 3x3x30 mm^3 normal 3x3x30 mm^3
Institute Laue Langevin, Grenoble, France, Dr. Bruno	on a line transverse to the seam, depth 2 mm; in-depth scan: 2 mm from weld edge	Neutron diffraction, strain scanner SALSA, 0.1768 mm, ~ 95^0	longitud. 3x3x3 mm^3, transverse 2x2x20 mm^3 normal 1x1x20 mm^3
Monash Univ., ANSTO Melbourne, Australia, Dr. Paradowska	on a line transverse to the seam, depth 3 mm,	Neutron diffraction, strain scanner TASS on HIFAR	longitud. 3x3x3 mm^3, transverse 3x3x20 mm^3 normal 3x3x20 mm^3
Rutherford Appleton Lab., Didcot, UK, Dr. Paradowska	on a line transverse to the seam, depth 3 mm and 15 mm; in-depth scan: along line1, Fig. 3	Neutron diffraction, ENGIN-X, ISIS Facility	longitud. 3x3x3 mm^3, transverse 3x3x20 mm^3 normal 3x3x20 mm^3

Table 2 Institutions using the semi-destructive or destructive measuring techniques: hole drilling method and deep hole drilling method. Different distances from the end of the plate for the various measurements. IHD = incremental hole drilling, DHD = deep hole drilling, E = 196 GPa, ν = 0.28

Measurements with destructive measuring techniques			
Institution	Measuring positions, distances from seam beginning	Measuring method, drilling device, drill diameter, hole depth	Hole diameter, strain gage rosettes (SGR), gage length, stress evaluation
TWI Great Abington, UK, Dr. Wei	on a line transverse to the seam: 110 or 125 mm from end of plate	abrasion jets for hole drilling, constant depth of holes ca. 1.9 mm	2.1 mm ∅, SGR, 1.59 mm length of individual gage
Paton Electric Welding Institute, Kiev, Ukraine, Prof. Lobanov	on lines transverse to the seam: 106, 116.5, 128 mm	constant depth of holes 1.0 mm	Electron speckle interferometry for measurement of strains,
Fraunhofer-Institut Werkstoff-mechanik, Freiburg, Germany, Dr. Pfeiffer	on a line transverse to the seam: 170 mm, mechanical polishing	IHD, high speed drilling device,	0.9 mm, SGR, MPA II differential method
CETIM, Senlis, France, Dr. Lieurade	measuring point 6 mm from weld centre line, 75 mm from weld beginning	IHD, milling machine, monobloc TC drill, 2 mm ∅,	strain gauges, E = 193 GPa, ν = 0.3
Materialprüfungsanstalt Universität Stuttgart, Germany, Dr. Kockelmann	on a line transverse to the seam: ca. 170 mm from weld beginning	IHD, high speed drilling turbine, 0.8 mm, 1.6 mm.∅	1,10; 1.82 mm ∅, SGR, 5.13 mm ∅, HBM/Kockelmann
Institut Füge/Schweißtechnik, Universität Braunschweig, Germany, Dr. Nitschke-Pagel .		IHD, micro measurements milling guide, hard metal drill,1.6mm∅	SGR, 5.13 mm ∅, Schajer method
Institute of Applied Mechanics Brno, Czech Republic, Dr. Slovacek,	on a line transverse to the seam:170 mm, polish.: emery paper	IHD, SINT high speed drilling device, TC drill, 1.4 mm ∅	SGR, EVAL RSM integral method and power series method
Institute for Materials Science, Welding and Forming, Graz University of Technology, Austria, Dr. Enzinger	on lines transverse to the seam: 100, 110, 120 mm	IHD, hard metal drill. 1.6 mm ∅.	1.66-1.87 mm ∅, SGR; 5.14 mm ∅, HBM/Kockelmann E=206 MPa, ν=0.3
Department of ;Mechanical Engineering, Unoverity of Bristol, UK, Prof. Smith	on lines transverse to seam: 65 mm 90 mm	IHD, DHD	

3. Results of residual stress calculations

3.1 Calculations according to the IIW programme "RSDP phase I and phase II"

As reported in section 2.2 the RSDP Round Robin has been started with 2D analyses. But due to the simplifications especially in the heat source modelling and in the 2D stress state the results of distortion and residual stresses have shown significant discrepancies and were not able to describe the real behaviour of the plate. The calculations have been followed with 3D calculations considering the moving heat source, the fitting of the heat input to measured thermocycles and temperature dependent material parameters given as input parameters to all participants. The kinematic material law was proposed and used in all calculations. As main results, it can be concluded that the temperature profiles calculated from the different partners show relatively small differences with a deviation in the peak temperature of some 20%, but in the residual stresses larger differences were found especially in the region close to the weld pool [9,10].

Fig. 7 shows the longitudinal residual stresses along line 3 from the centreline of the weld via the heat affected zone to the plate surface. The longitudinal stresses show tension in the weld with peak stresses between 250 and 300 MPa followed by a transition zone whereas the width of this zone deviates in the results from the different partners. The transverse residual stresses on the other hand (**Fig. 8**), show larger discrepancies in the region of interest in the weld material and the neighbouring heat affected zone. In the centreline of the weld the stress results vary from compression to tension and therefore also in a region up to 30 mm from the weld centreline significant differences in the results from the different participants are obtained.
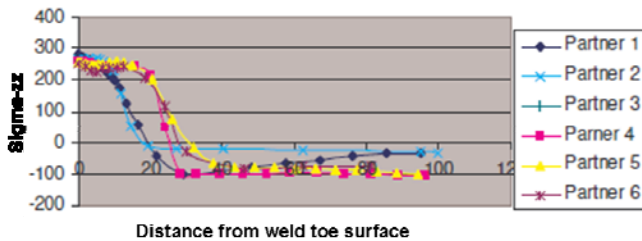

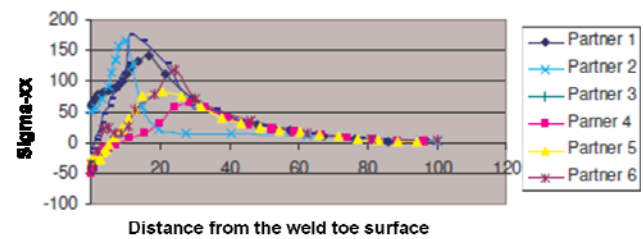**Fig. 7** Longitudinal residual stresses along line 3, 3D-calculation with the material law of kinematic hardening [9,10]

Fig. 8 Transverse residual stresses along line 3, 3D-calculation with the material law of kinematic hardening [9,10]

3.2 Additional calculations with different strain hardening approaches

As already mentioned, the additional new calculations have been performed in order to clarify whether the use of other hardening rules than proposed in the RSDP programme (phase II) could provide a better agreement with the results of measurements, especially indicating also maxima of the longitudinal residual stresses in the HAZ.
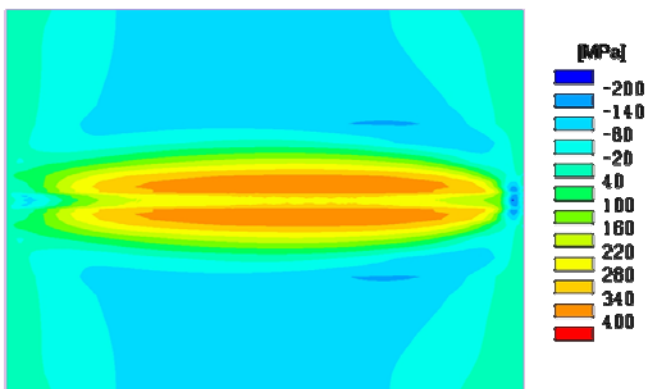

Fig. 9 Longitudinal residual stresses (nodal solution) at the top side of the welded austenitic steel plate, 3D-calculation with the material law of isotropic hardening, [11]
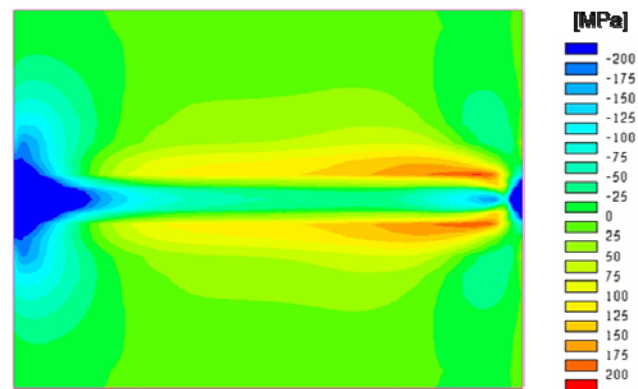
Fig. 10 Transverse residual stresses (nodal solution) at the top side of the welded austenitic steel plate, 3D-calculation with the material law of isotropic hardening [11]

Fig. 9 and **Fig. 10** represent calculated distributions of longitudinal and transverse residual stresses in the surface layer of the austenitic steel plate. A purely isotropic hardening model was used for the calculations referring to the state after welding of the second pass. The distribution of longitudinal residual stresses at nodes in **Fig. 9** reveals clearly a lower magnitude (about 270 MPa) of the tensile residual stresses along the weld centre line in comparison with maximum magnitudes of 380 MPa on both sides of the weld seam [11].

Fig. 10 indicates that the distribution of transverse residual stresses is not symmetrical with regard to a centreline transverse to the weld seam. The maxima of tensile residual stresses are closer to one end of the seam. This result may be a consequence of the continuous welding process beginning at one end of the plate. Along the middle of the seam a rather broad band of compressive residual stresses with a magnitude of about -50 MPa is noticeable, which is surrounded on both sides by tensile residual stresses with magnitudes up to more than 150 MPa.
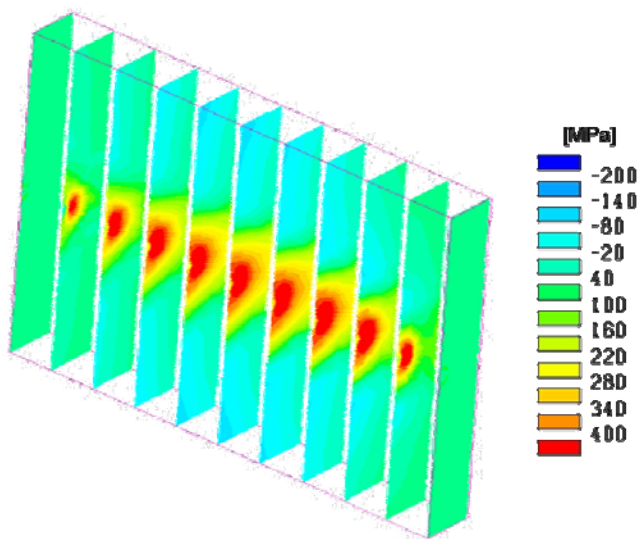
Fig. 11 Longitudinal residual stress distributions over various cross sections calculated with the material law of isotropic hardening [11]
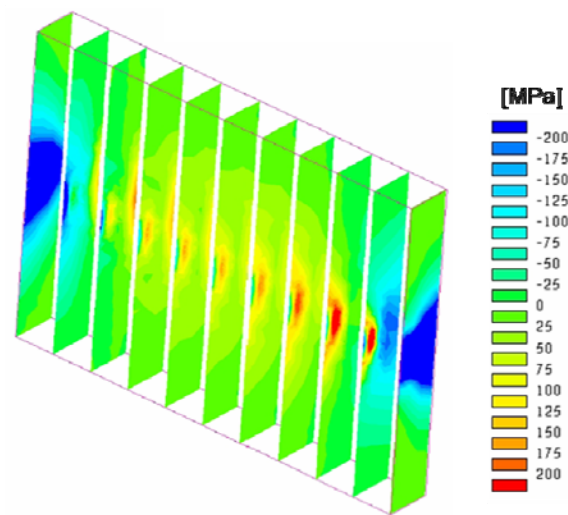
Fig. 12 Transverse **r**esidual stress distributions over various cross sections calculated with the material law of isotropic hardening [11]

The distribution of longitudinal residual stresses over various cross sections in **Fig.11** indicates high tensile residual stresses in the range of 400 MPa also in deeper layers, whereas tensile residual stresses (**Fig. 12**) in the transverse direction reach only a smaller depth below surface.

For comparisons (and further discussions) plots of residual stress values versus distance from the weld centre line are used in the following. The next figures represent such distributions of calculated longitudinal and transverse residual stresses along a line transverse to the weld seam in a distance of 180 mm from the weld start. The characteristic features of all distributions of longitudinal residual stresses calculated with a pure or partly isotropic strain hardening model show minima at the weld centre line with magnitudes of ca. 270 MPa and maxima in a distance of approximately 8 mm from the weld centre line with various magnitudes, **Fig. 13**.
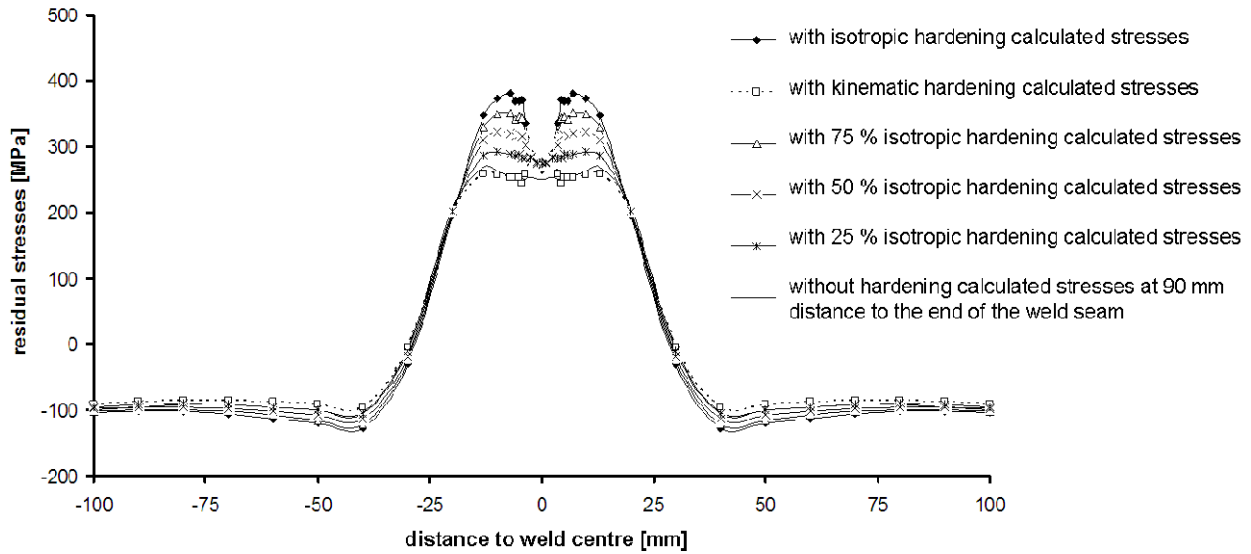
Fig. 13 Longitudinal residual stresses at nodes versus distance from the weld centre line calculated with various different material laws [7]
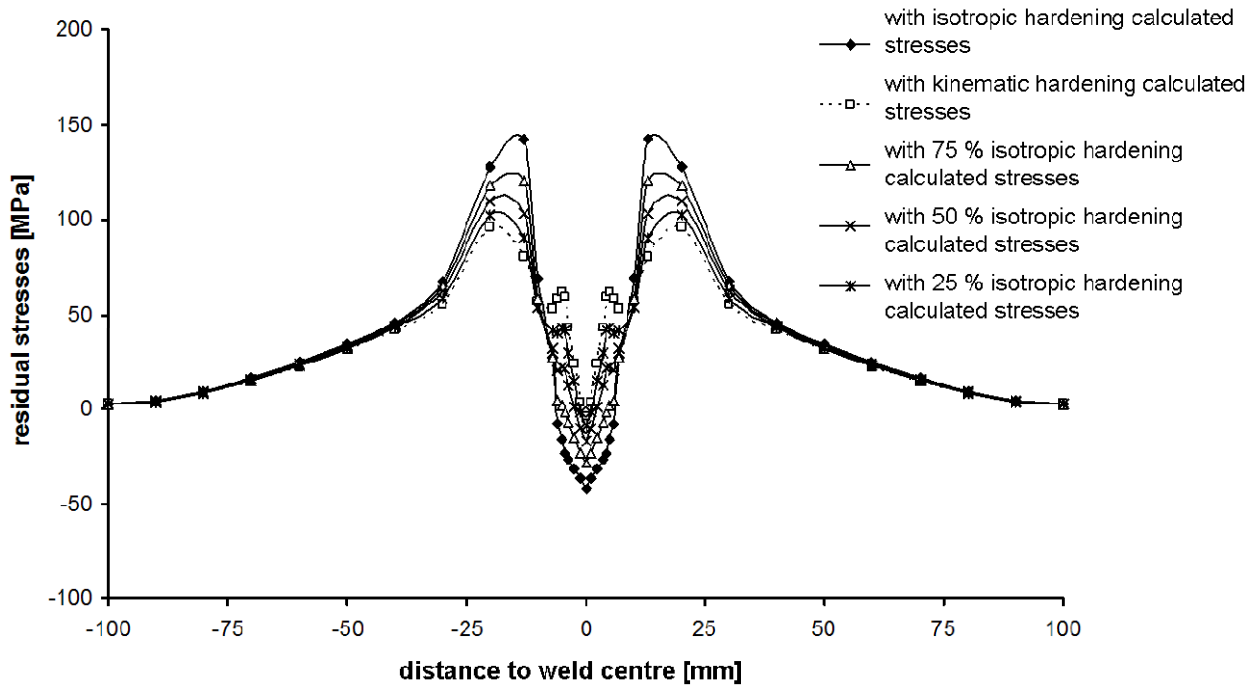

Fig. 14 Transverse residual stresses versus distance from the weld centre line calculated with various different material laws [7]

It is clearly visible that the magnitudes of the maxima decrease with an increasing percentage of kinematic hardening in the model assumptions, from ca. 380 MPa in calculations with a pure isotropic hardening model down to ca. 300 MPa of a rather weak maximum in calculations with the assumption of 75% of kinematic hardening. Calculations with a pure kinematic hardening model result in a nearly horizontal distribution of maximum longitudinal stresses of ca. 250 MPa over the weld seam and adjacent areas, practically the same result as with calculations using an ideal elastic-plastic material behaviour.

Distributions of transverse residual stresses calculated with various material laws are illustrated in **Fig. 14**. The assumption of pure isotropic hardening results in the highest tensile stress maxima of about 150 MPa in a distance of ca. 10 mm from the centre line in comparison with lower stress maxima if the calculation models contain percentages up to 75 % of kinematic hardening. The stress minimum at the weld centre line is with -50 MPa most pronounced under the assumption of pure isotropic hardening. Calculation models containing different percentages of kinematic hardening result in stress minima with lower magnitudes in the compressive range at the centre line.

4. Results of residual stress measurements

As can be seen in **Table 1** and **Table 2** quite a number of institutions has carried out measurements of the residual stresses of one of the test plates with various techniques and different methodologies. Typical results of each measuring technique will be illustrated in the following figures. The figures are supplemented by **Table 3** in order to present as much as possible of the entity of all results, which cannot be shown in detail. Results which do not agree with the illustrated main tendencies will be especially mentioned [8, 12, 13].

4.1 Distributions of residual stresses versus distance from the weld centre line, measurements integrating over a distinct depth

4.1.1 Non-destructive measurements

Non-destructive measurements have been carried out in laboratories A, B, I and L by means of X-rays and in laboratories G, H, N and P with the neutron diffraction method. Individual measuring conditions are summarized in **Table 1**. An important feature of each method is the "integration volume" over which an averaged value of the locally varying residual stresses is taken and if stress gradients versus depth are to be anticipated especially the "integration depth" as the thickness of the layer over which the varying stresses are integrated. It must be emphasized that the integration depth of the X-ray method is only 10 μm, that is to say extraordinary low in comparison with all other methods. The incremental hole drilling technique for instance uses a first step with a depth of 0.02 mm or of 0.05 mm, whereas in neutron diffraction the integration depth is for instance 3 mm.

Typical residual stress distributions taken by X-ray diffractometry are shown in **Fig. 15**. They are characterised by the stress minima at the weld centre line, ca. -150 MPa for the transverse stress component and ca. +300 MPa for the longitudinal component, and by pronounced tensile stress maxima in the HAZ, +300 MPa in the transverse stress distribution and +500 MPa in the distribution of longitudinal stresses in distances of ca. 10 mm and 6 mm to 8 mm from the centre line, respectively. In larger distances from the weld the residual stresses decrease to lower values, which are rather inconsistent in different measurements. In can be concluded that this inconsistency in areas more remote from the weld is rather a consequence of foregoing machining operations, which induce stresses in a very thin surface layer of the plate, than of the heat input due to welding (**Fig. 15**).
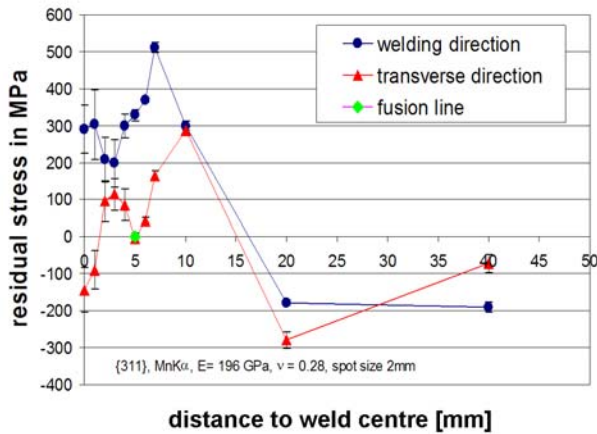
Fig. 15: X-ray results, laboratory A, plate I. Distribution of longitudinal and transverse residual stresses measured over a depth of ca. 10 μm [8]
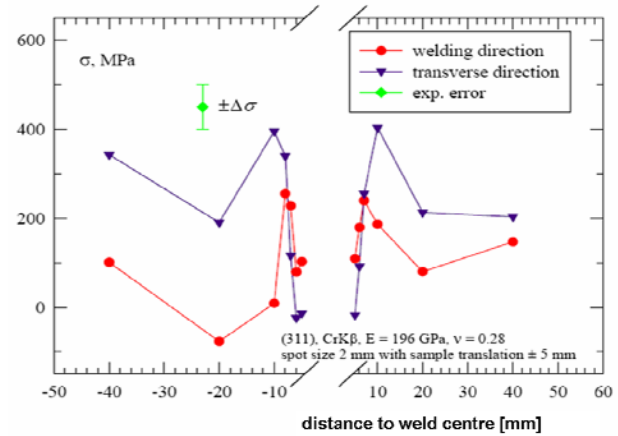
Fig. 16: X-ray results, laboratory I, plate II. Distribution of longitudinal and transverse residual stresses measured over a depth of ca. 10 μm [12]
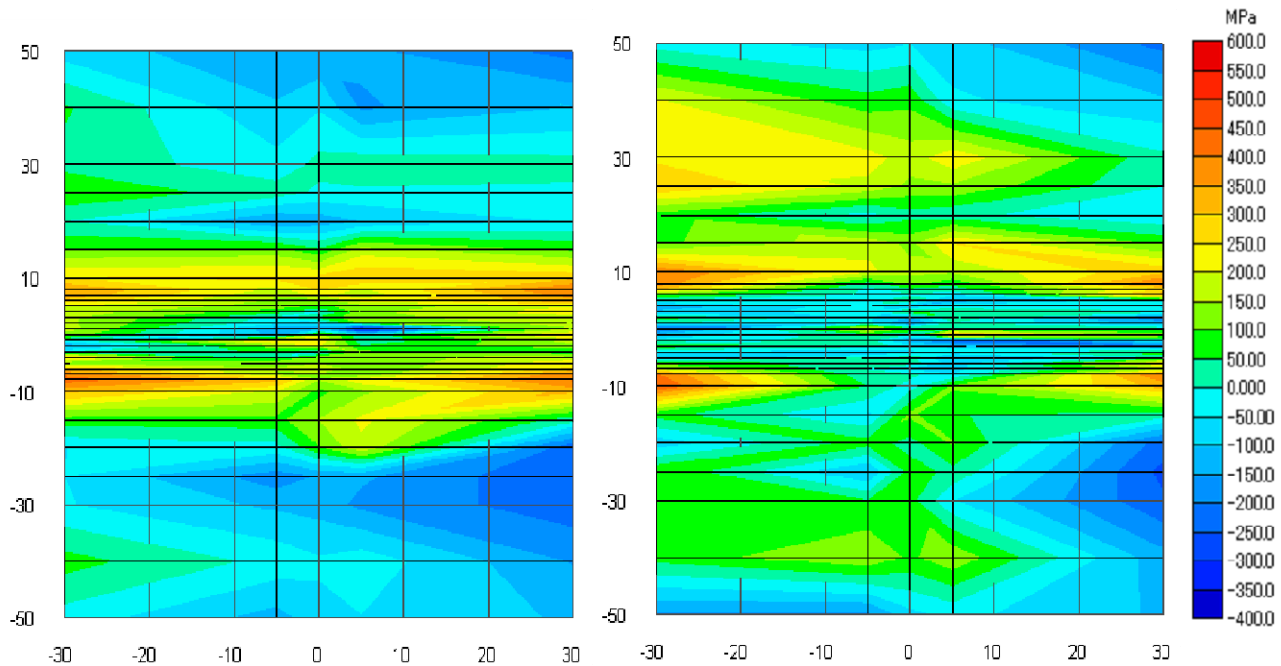

Fig. 17 Planar illustration of residual stresses measured by means of X-rays, laboratory L, plate I, longitudinal stresses (left), transverse stresses (right) in MPa over the distance from the centre of electrochemical polished area in mm [13]

The results of other measurements by means of X-rays offer a qualitative confirmation of the mentioned results with the same pattern of minima at the weld centre and maxima in the HAZ. The results of laboratory I show also sharp stress maxima in the HAZ, but the maximum magnitudes of longitudinal and transverse stresses look like exchanged, **Fig 16**. Laboratory L on the other side has provided a laminar illustration by measuring the stresses along five lines transverse to the seam in distances between 20 mm and 66 mm from the beginning of the seam, **Fig. 17**. Minimum magnitudes and partly compressive stresses along the weld centre and areas with maximum magnitudes more outside are clearly to be seen. Possibly the quantitative differences between the results of laboratories

I, L and laboratories A, B can be a consequence of the fact that measurements have been carried out in rather different distances to the beginning of the weld seam (see **Table 3**).

The residual stress distributions taken by neutron diffraction reveal also the same characteristics: relative stress minima at the weld centre line and tensile stress maxima in certain distances from the centre line. However the maxima are less pronounced than in the X-ray measurements, for instance +100 MPa for the transverse stress component and +300 MPa for the longitudinal component, as can be seen in typical stress distributions in **Fig. 18**. In connection with these results one has to keep in mind that the neutron diffraction measurements evaluate stress values averaged over a depth of 3 mm. In the longitudinal stress distributions balancing compressive stresses can clearly bee seen in distances bigger than 25 mm respectively 30 mm from the weld centre line. The magnitudes of the transverse stresses beyond the weld seam, as well as the normal stresses, remain in a very low range over the whole width.
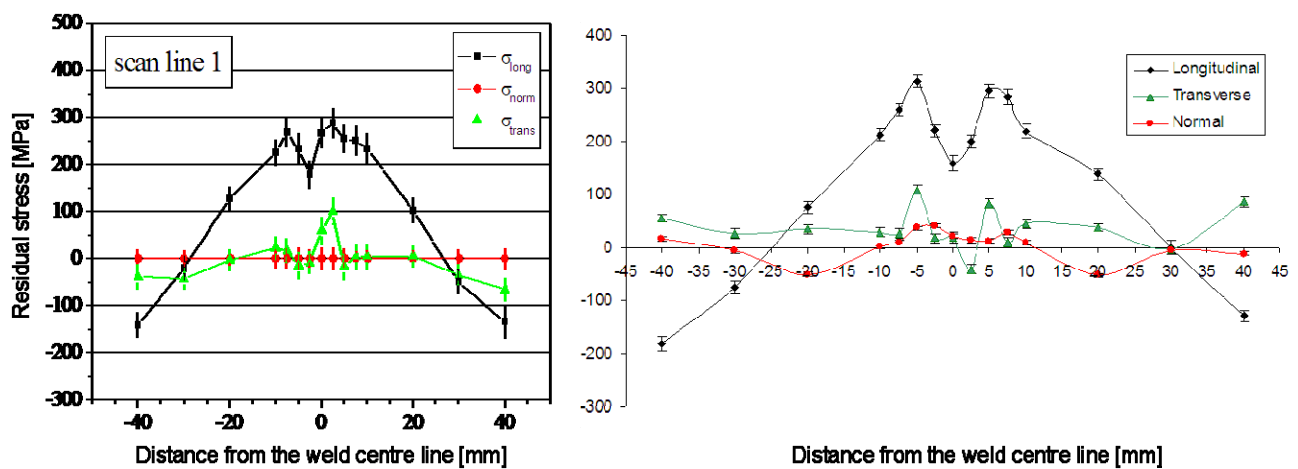

Fig. 18 Results of neutron diffraction, laboratory H (left) and P (right), plate I, measuring depth 3 mm [12, 13]

4.2.2 Semi-destructive measurements

Two institutions used the hole drilling method in order to find residual stress distributions versus distance from the weld centre line. At each measuring point the measured stresses are integrated over a distinct depth below surface.

Laboratory K used measuring lines transverse to the seam in distances of 110 mm respectively 125 mm from the end of the seam. The results reported in **Fig. 19** indicate maxima of the longitudinal stress component of 356 MPa respectively 327 MPa in distances of 7.5 mm from the centre line on both sides of the seam. At the weld centre line the longitudinal stresses attain a minimum value of 255 MPa on the top side of the plate (side A). The transverse component shows nearly constant values between 135 MPa and 167 MPa. The longitudinal stresses measured on the back side (side B) indicate a maximum magnitude at the weld centre line (235 MPa) and a lower stress value in a distance of 7.5 mm from the centre line, the transverse stresses are nearly identical on this side of the plate.

The technique of laboratory M is a sophisticated variant of the hole drilling method using electron speckle interferometry for the measurement of deformations during hole drilling. The measurements are taken along lines transverse to the seam in distances of 106 mm, 116.5 mm and 128 mm from the end of the seam and the integration depth of each measured stress value was 1.0 mm in this case. The

results in **Fig. 20** reveal again tensile maxima of the longitudinal stresses between 346 MPa and 410 MPa in distances of 7.5 mm from the centre line and minima at the centre line between 191 MPa and 293 MPa. Two courses of transverse stresses show distinct minima in the compressive range at the centre line, the third course does not exhibit such a minimum, but nearly the highest tensile stress at the centre line.
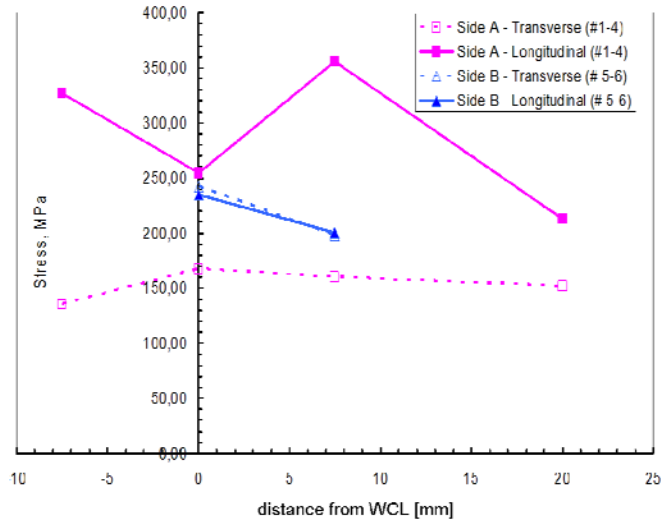

Fig. 19 Hole drilling results, laboratory K, plate III, residual stresses averaged over a depth of 1.9 mm [12]
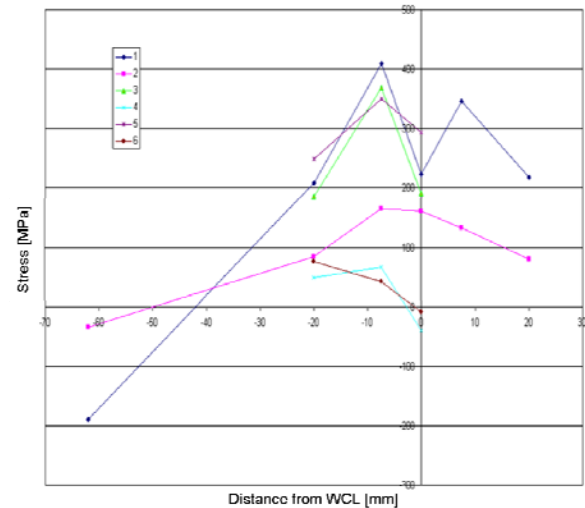
Fig. 20 Electron speckle-interferometry after hole drilling, laboratory M, plate III, residual stresses averaged over a depth of 1.0 mm [13, 14, 15]

In order to indicate the main results of the measurements and even some contradiction, in **Table 3** magnitudes of the longitudinal and transverse residual stresses are summarized which have been measured at the weld centre line, in the important positions between 6 mm and 8mm from the centre line and in a distance of 20 mm from the centre line. Additional to the magnitudes measured by means of X-rays and with neutron diffractometry also results found with the first step of the incremental hole drilling method are listed. These values of the hole drilling technique close to the surface can give a useful completion and also some confirmation of the residual stress values measured for instance by means of X-rays at the weld centre line, although the hole drilling technique may produce errors due to the necessary polishing of the surface of the weld seam. But X-ray measurements at the top of the weld seam are also difficult and connected with rather big measuring errors.

As one can see in **Table 3** most of the stress values measured by means of incremental hole drilling underline the existence of a relative minimum at the weld centre line and are also a good confirmation of stress maxima in a distance between ca. 6 mm and 8 mm from the centre line, even if individual values are not in accordance with this tendency. The differences of results of X-ray measurements of the laboratories I and L have been discussed already in the foregoing chapter and it has been mentioned, that they also underline the tendency of maxima in the HAZ and a minimum close to the weld centre line (**Fig. 16** and **Fig. 17**).

Finally all measurements of the longitudinal stress component reveal rather clear patterns, very close to the surface (X-ray, incremental hole drilling) and also in deeper layers (hole drilling, neutron diffraction): a relative minimum of tensile stresses at the weld centre line and tensile stress maxima in the HAZ in a distance of 6 – 8 mm from the centre line. Considering the magnitudes of the maxima a clear tendency can be observed: these magnitudes are obviously higher in layers very close to the surface and decrease with the measuring depth. The magnitudes in layers very close to the surface (X-ray, incremental hole drilling) are mainly in the range between 400 MPa and 500 MPa

(mean value 477 MPa, with exception of laboratory I and L) whereas in a measuring depth of 1.0 mm or 1.9 mm (hole drilling method with constant hole depth, laboratories K and M) the magnitudes are in the range between 320 MPa and 410 MPa (mean value 358 MPa) and in measuring depths of 2.0 mm and 3.0 mm (neutron diffraction) the lowest magnitudes between 270 MPa and 370 MPa (mean value 309 MPa) have been found. For the minima at the weld centre line such a tendency cannot be observed. With some exceptions these minima remain at medium magnitudes. With the exception of X-ray measurements all results demonstrate balancing compressive longitudinal stresses in distances bigger than 25 mm to 30 mm from the centre line.

The transverse stresses show (with two exceptions) minimum magnitudes at the weld centre line, often in the compressive range or close to zero. Transverse stress distributions measured by means of X-rays or with the hole drilling method indicate in principle similar patterns as the longitudinal stresses, but with smaller minima at the centre line or minima in the compressive range (see **Table 3**) and smaller maxima in the HAZ . The values measured in the HAZ (10 mm from the weld centre line) with the incremental hole drilling method are rather inconsistent and cannot confirm the maxima.

Table 3: Magnitudes of longitudinal and transverse residual stresses measured with the different techniques at the weld centre line and in distances of 6 to 8 mm or 10 mm as well as in 20 mm from the weld centre line. Stress magnitudes in MPa. Results in brackets are obtained under somewhat differing conditions.

Labor, method, integration depth, plate number	At (or close to) the centre line		6 to 8 mm (long.) or 10 mm (transv.) from the centre line		20 mm from the centre line	
	longitud. stress	transverse stress	longitud. stress	transverse stress	longitud. stress	transverse stress
A, X-ray, 10μm, I, II	290, 302	-144, (-71)	512, 495	287. 361	-178, 86	-279, -6
B, X-ray, 10 mm, III			428, 430	356		
I, X-Ray, 10 μm, II			255, 240	396, 404	-77, 80	191, 213
L, X-Ray, 10 μm, I	(-116)	(-183)	(258, 269)	167, -22	-133, 96	29, 33
A, incr. hole dr., II	200	0	540	110	-10	-50
B, incr. hole dr., III	150		580	170		
C, incr. hole dr., II	150	-115	492, 563	14, 49	289	34
D, hole drill, 0.02, II	262	-27	480	56	78	-44
E, incr. hole dr., II	480	20	380 - 480	80 – 90	0 – 100	-270 - 0
F, incr. hole dr., II	-50, 350	-60, 70	0, 350	-20, 150	-80, -120	-120, -230
M, hole.dr.,1.0 mm, III	191 - 293	-40 - 157	346 - 410	(43 – 165)	218	81
K, hole dr., 1.9 mm, III	255	167	321, 356	(135, 160)	213	152
G, neutr. diffr.,2mm,III			280	260	220	140
H, neutr.diffr., 3mm,I	180	0	270, 290	100	120	0
N, neutr. diffr., 3mm, I	180	0	330, 370	100	160	70
P, neutr.diffr., 3mm, I	160	20	300, 320	80 – 100	80 - 140	30 - 40

According to measurements versus distance from the centre line in a depth of 15 mm with neutron diffraction techniques the longitudinal residual stresses show a maximum magnitude between 180 MPa (laboratory H) and 230 MPa (laboratory P, **Fig. 21**) in the position below the centre line and decrease down to zero in a distance of ca. 25 mm and in bigger distances from the centre line to compressive stresses. The magnitudes of the transverse stresses below the centre line are 100 MPa in the compressive range and decrease to zero respectively change into the tensile range with increasing distance from the centre line.
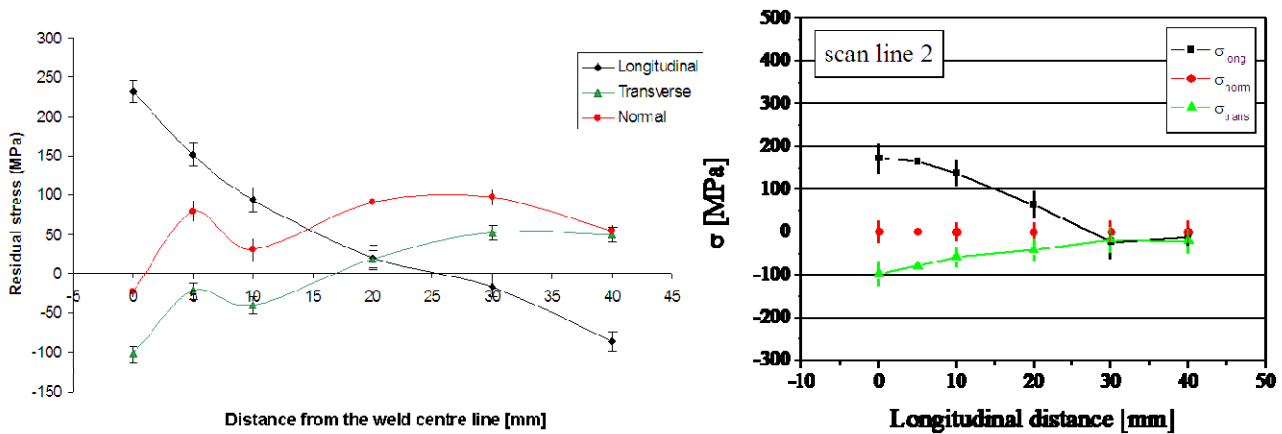
Fig. 21 Results of neutron diffraction, laboratory P (left) and H (right), plate I, residual stresses versus distance from the centre line in a depth below surface of 15 mm [12, 13]

4.2 Distributions of residual stresses versus depth below surface

Typical for the incremental hole drilling method are evaluations of the residual stresses at distinct positions down to a depth in the range of 1 mm. Consequently such measurements offer information about the residual stress gradients in surface layers of an appropriate thickness. Information about the residual stress field in deeper layers respectively about the course of residual stresses down to deeper layers have been taken with other techniques like neutron diffraction or the deep hole drilling method.

4.2.1 Measurements with the hole drilling method, depth values <1.2 mm [12]

Examples of residual stress distributions versus depth below surface at selected positions are illustrated in **Fig. 22** to **Fig. 26**. At the same distances to the centre line the magnitudes of measurements close to the surface are obviously within a reasonable scatter band, as already shown in **Table 3**. But the courses of longitudinal residual stresses versus depth below surface under the weld centre line show some inconsistencies: longitudinal stresses with strongly increasing magnitudes versus depth below surface have been evaluated (**Fig. 22**) as well as nearly constant or slowly decreasing (**Fig. 23**) longitudinal stresses.

But as inscribed in **Fig. 22**, the very low magnitudes of longitudinal and transverse stresses measured by laboratory A very close to the surface may be a consequence of mechanical polishing, which was especially necessary on the uneven surface of the seam. Due to general experience the mechanical polishing could have changed the original stress values in the direction of compressive stresses and the rather steep increase of longitudinal stresses in layers very close to the surface would become understandable in this case – and also in other cases.

At the position of the maxima of longitudinal residual stresses in distances between 6 mm an 8 mm from the weld centre line the results of the different laboratories are really consistent. A decrease from the high maximum tensile stresses close to the surface was observed towards deeper layers in all measurements. This decrease is followed by a new, small increase of the magnitudes towards the final depth (**Fig. 24**). A comparison of the results of laboratory E indicates that the increment of the drilling depth may have a substantial influence on the stress distribution.
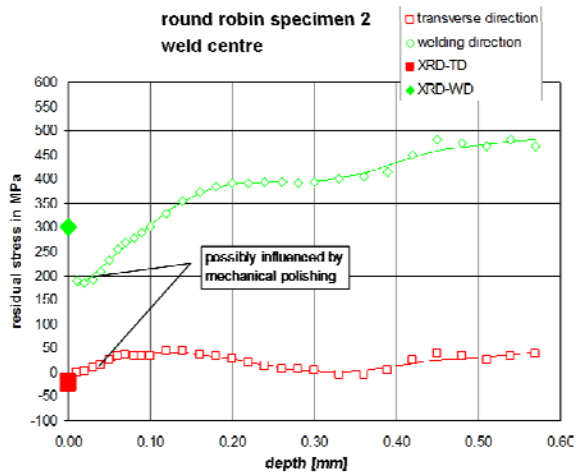
Fig. 22 Incremental hole drilling results, laboratory A, plate II, residual stresses versus depth below surface at the weld centre line, (170 mm from seam end) [8]
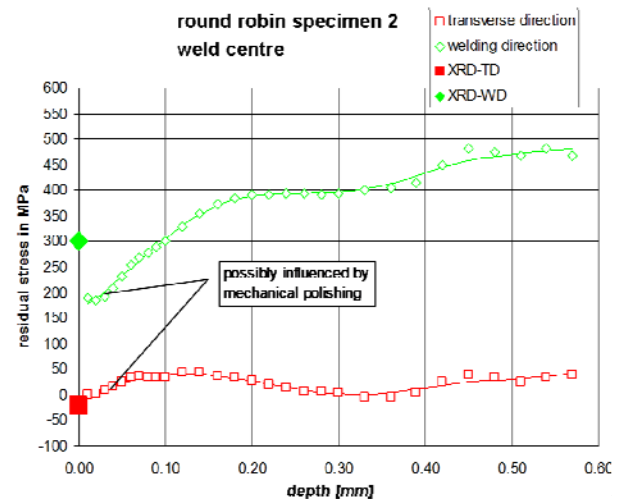
Fig. 23 Incremental hole drilling results, laboratory C, plate II, residual stresses versus depth below surface at the weld centre line, (ca.200 mm from seam end) [12]
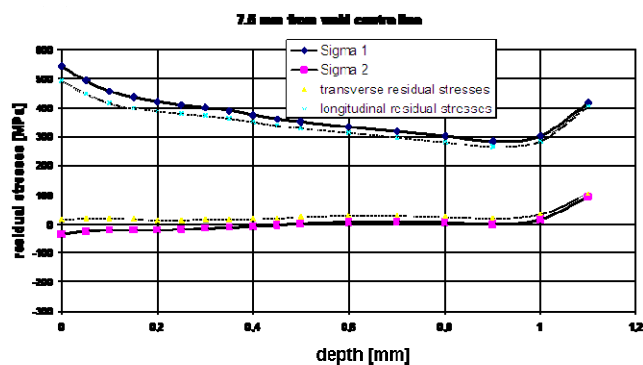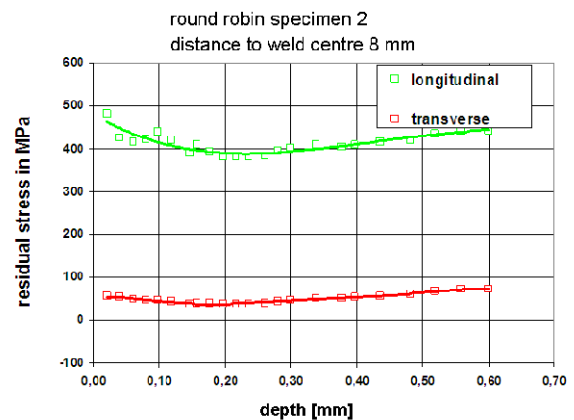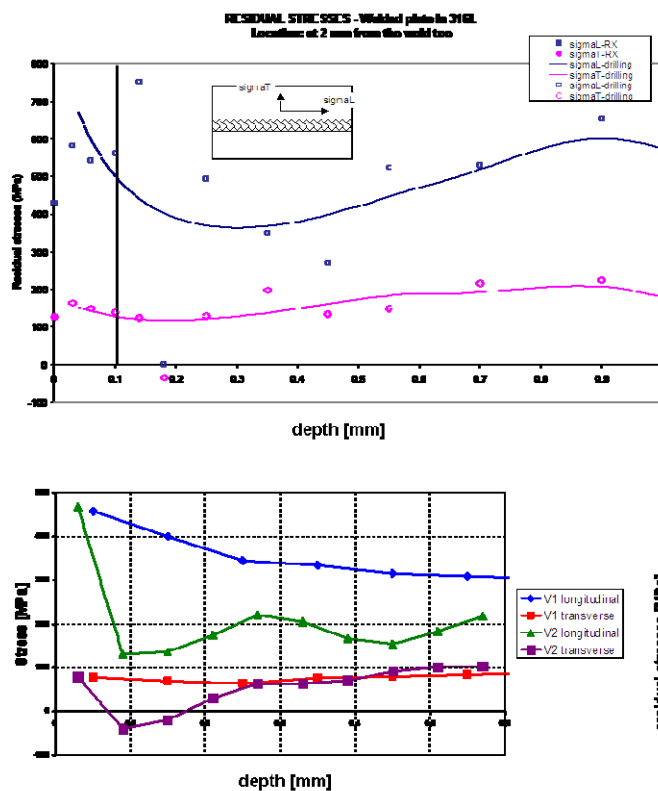

Fig. 24 Incremental hole drilling results, laboratories B (upper left, plate III), C (upper right), D (lower left), E (lower right), plate II, residual stresses versus depth below surface at a distance of ca. 6 mm from the weld centre line [8,12]

In a distance of 20 mm from the centre line the rather low longitudinal residual stresses show in most measurements, with the exception of the first values close to the surface, nearly constant magnitudes of 150 MPa or ca. 200 MPa over a wide depth range (**Fig. 25**). The steep increase of stresses close to the surface in two cases could again be a consequence of mechanical polishing.
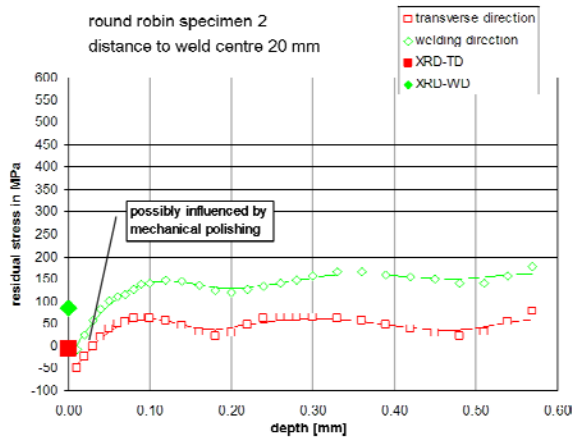
Fig. 25 Incremental hole drilling results , laboratory A plate II, residual stresses versus depth below surface at a distance of ca. 20 mm from the weld centre line [12]
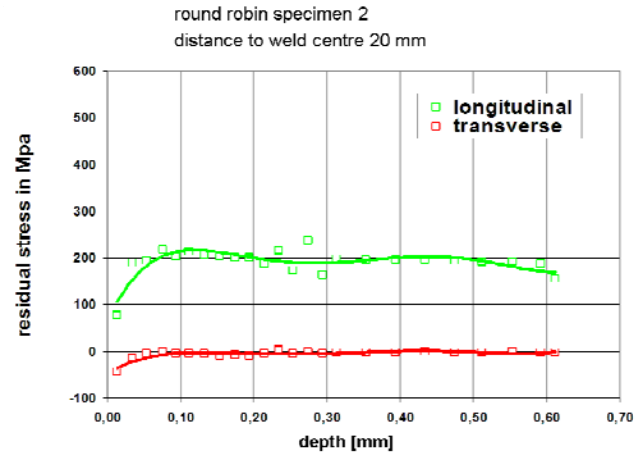
Fig. 26 Incremental hole drilling results , laboratory C plate II, residual stresses versus depth below surface at a distance of ca. 20 mm from the weld centre line, (ca. 200 mm from seam end) [12]

The rather small magnitudes of the transverse residual stresses remain nearly constant versus depth below surface – under the weld centre line mainly in the compressive range and at positions between 6 mm and 8 mm from the centre line mostly in the tensile range between 50 MPa and 200 MPa (**Fig. 22** to **Fig. 24**). Also in a distance of 20 mm from the centre line the courses of the transverse stresses versus depth below surface are nearly constant with small magnitudes either in the tensile or in the compressive range, **Fig. 25** and **Fig. 26**.

4.2.2 Measurements with neutron diffraction and with the deep hole drilling technique, depth values >1.2 mm

With the neutron diffraction technique longitudinal and transverse stress components have been measured versus distance from the surface to a depth of maximal 27 mm and also along line scans transverse to the seam in a depth of 15 mm. Measurements of the longitudinal stress component versus depth under the weld centre line indicate an increase of tensile stresses up to magnitudes of ca. 230 MPa or 370 MPa in layers of 6 mm respectively 15 mm below surface (**Fig 27** and **Fig. 28**).
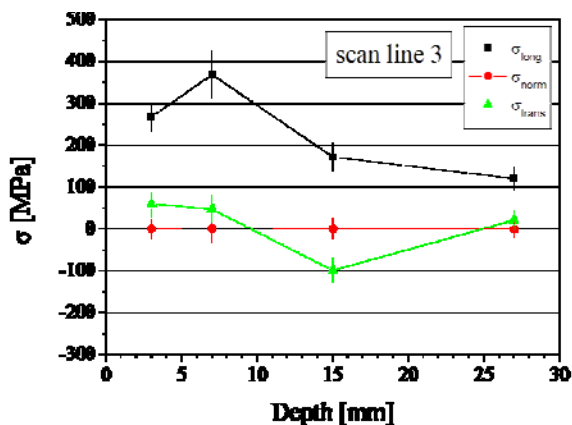

Fig. 27 Neutron diffraction results, laboratory H, plate I, residual stresses versus depth below surface at the weld centre line, (170 mm from seam end) [12]
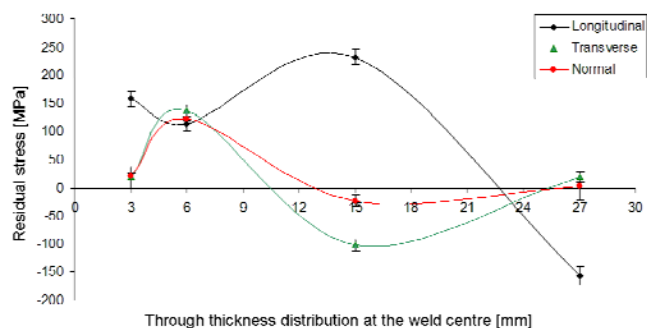
Fig. 28 Neutron diffraction results, laboratory P, plate I, residual stresses versus depth below surface at the weld centre line [13]

According to these measurements tensile residual stresses are still present in layers of more than 20 mm below surface. With the deep hole drilling method a principally similar distribution of the longitudinal stress component versus depth below surface, with a maximum magnitude of somewhat more than 250 MPa in a depth of ca. 6mm, has been evaluated (laboratory Q, **Fig. 29**). In-depth measurements at the position 6 mm from the weld centre line (laboratory G, **Fig. 30**) revealed also tensile longitudinal stresses between 200 MPa and 300 MPa in a depth between 2 mm and 6 mm which are slowly decreasing from 6mm to 10 mm depth.
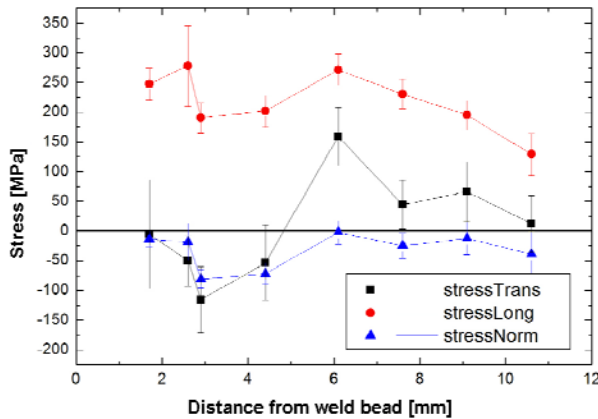

Fig. 29 Results of the deep hole drilling method, Laboratory Q, plate III, longitudinal residual stresses versus depth below surface at the weld centre line [13]
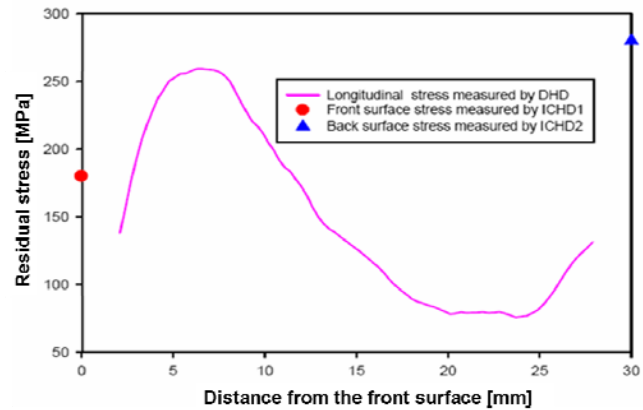
Fig. 30 Neutron diffraction results, laboratory G, plate III, residual stresses versus depth below surface in a distance of 6 mm from the weld centre line [12]

4.3 Results of additional investigations

4.3.1 Calculated Deformations of the plate due to welding

In addition to the residual stress evaluations also the bending around the weld axis (angular distortion) as well as around an axis transverse to the weld seam have been measured and calculated at the Fraunhofer-Institut für Werkstoffmechanik, Freiburg. **Fig. 31** and **Fig. 32** illustrate the measured distortions in comparison with different calculations. As can be seen in the figures, the bending around an axis transverse to the weld (**Fig. 31**) is much less pronounced - nearly negligible – in comparison with the angular distortion (**Fig. 32**). The differences between the measured and the calculated values are rather small. The influence of the dead and birth technique of the filler material with respect to the displacements due to welding is negligible (**Fig. 31**).

4.3.2 Metallographic investigations

Hardness measurements with different loads (HV0.2, HV 1, HV 5) along lines transverse to the weld seam showed rather constant values in the seam and in the HAZ [16]. Neither significantly lower hardness values in the weld seam nor really significant hardness maxima in a distance of the weld seam could be observed.

According to [17] a certain content of δ-ferrite to avoid hot cracking phenomena has to be anticipated in the weld seam. This fact was supported by additional metallographic inspections, that have revealed a dendritic structure in the weld seam with some amount of δ-ferrite [16].
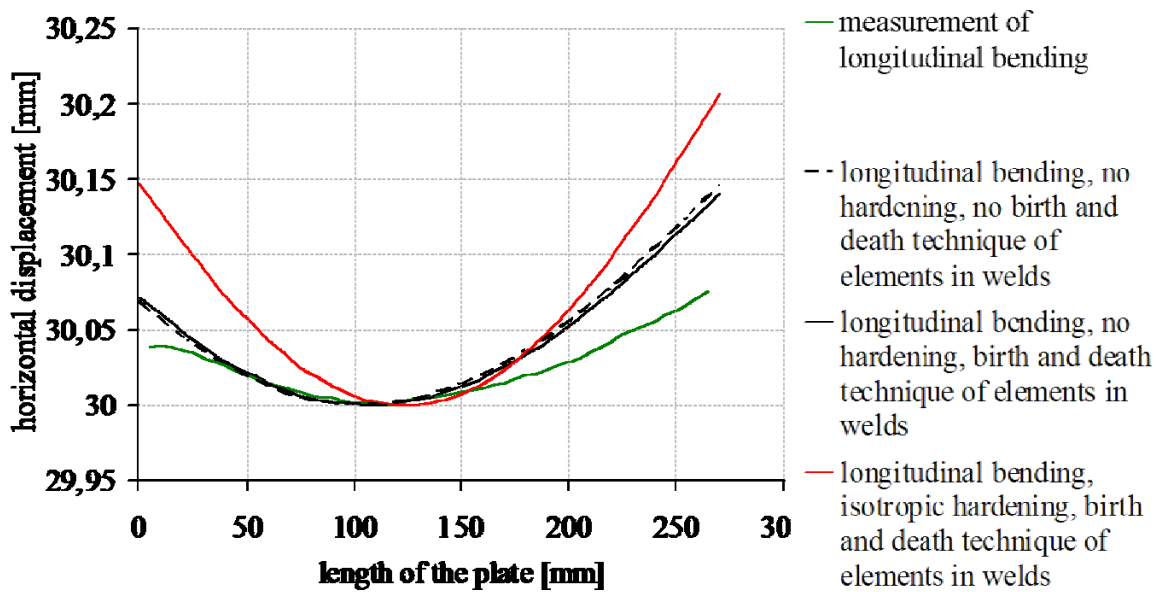
Fig. 31 Measured and calculated longitudinal bending around an axis transverse to the weld [18]
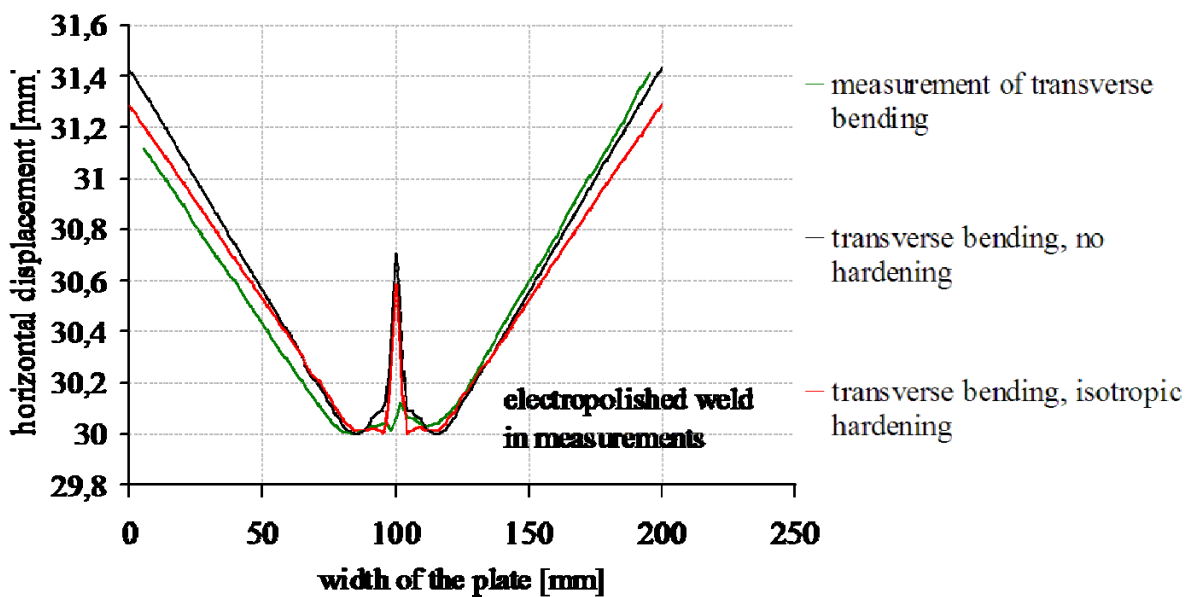
Fig. 32 Measured and calculated angular distortion (transverse bending around the weld axis) [18]

5. Discussion

5.1 Comparison of calculated and measured residual stress distributions

The main discrepancy between the older calculations with the assumption of kinematic hardening and the newer ones with the assumption of isotropic hardening concerns the distribution of the longitudinal residual stresses. The older calculations demonstrate a rather flat, horizontal course of longitudinal tensile stresses in areas close to the weld seam, partially with a weak maximum at the centre line with magnitudes in the range of the yield strength of the base material (approx. 250 MPa).

In a distance of 15 to 25 mm from the centre line the longitudinal stresses decrease and change to compressive stresses, **Figs. 7** and **13**. Contrasting with this result the new calculations with the model of isotropic hardening indicate longitudinal residual stresses with a minimum of tensile stresses in the range of the yield strength at the weld centre line (approx. 270 MPa) and distinct maxima with magnitudes of ca. 380 MPa in a distance of approx. 8 mm from the centre line. It is obvious that the results of the older calculations do not agree with the reported measured pattern of longitudinal stresses. On the other side, the agreement of longitudinal stress distributions calculated under the assumption of isotropic hardening with measured ones becomes nearly perfect if measurements and calculations with the same integration depth of stresses are compared, as well with regard to the magnitudes of the maxima as also with regard to their position. **Fig. 33** approves this statement, calculations and measurement**s** by means of the hole drilling method in connection with electron Speckle-interferometry are compared.

Comparison of the new calculations and the measurements of transverse residual stresses in **Fig. 34** indicates a situation which is not as clear as for the longitudinal stresses. Only two of the measured residual stress distributions show stress minima in the compressive range at the weld centre line and are therefore in agreement with the calculated stresses. But the measurement in a distance of 128 mm from the end of the weld seam indicates a tensile stress maximum of more than 150 MPa at the weld centre line. This discrepancy to the other measured results could possibly be a consequence of the different distances of the measurements to the end of the seam because the distribution of the transverse residual stresses is asymmetric as already shown in **Fig. 10**. In addition it should be mentioned that other measurements by means of X-ray diffraction or neutron diffraction exhibited also tensile stress maxima of 300 MPa or at least 100 MPa in distances of ca. 10 mm from the weld centre line and a stress minimum in the compressive range at the weld centre line [8, 12, 13] and support therefore the calculated result in principle.

It should be also mentioned here, that distributions of transverse residual stresses computed by using the kinematic hardening model or the isotropic hardening model do not show fundamental qualitative discrepancies, however noticeable quantitative discrepancies.
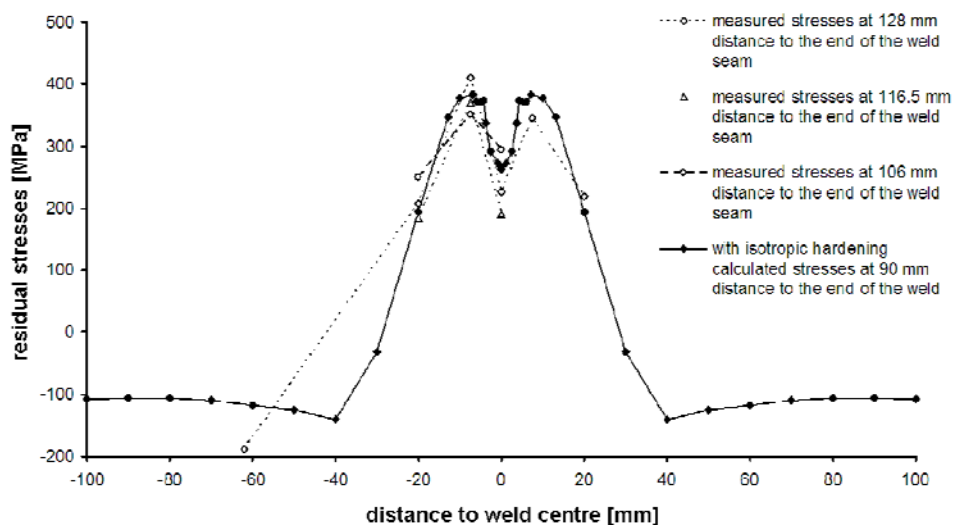

Fig. 33 Longitudinal residual stresses measured by means of hole drilling and electron Speckle-interferometry (stresses averaged over a depth of 1 mm, laboratory M in the IIW Round Robin Programme) in comparison with calculated longitudinal residual stresses (isotropic hardening, element size 1 mm^3), [7]
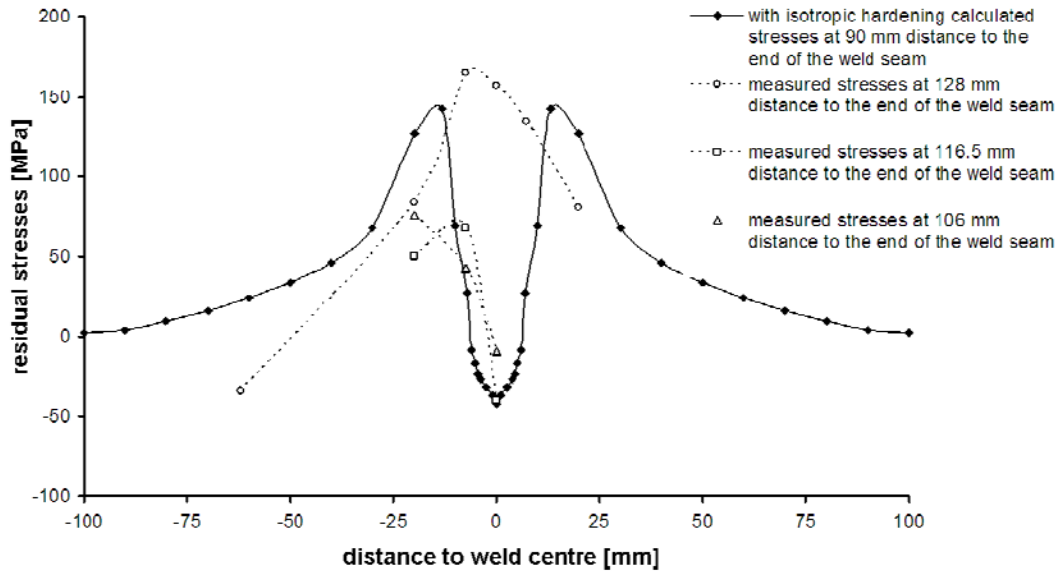
Fig. 34 Transverse residual stresses measured by means of hole drilling and electron Speckle-interferometry (stresses averaged over a depth of 1 mm, laboratory M in the IIW Round Robin Programme) in comparison with calculated longitudinal residual stresses (isotropic hardening, element size 1 mm^3, [7]

5.2 Discussion about the calculated stress maxima and the differences between calculations with different strain hardening models

Consequently important points of the discussion have to be whether explanations for the maxima and minima of the longitudinal residual stresses can be given and why the maxima can not be found by calculations with a kinematic hardening model. Considerations which are able to explain both effects of the calculations – the existence of the calculated maxima and minima as well as the difference between the two calculation models – are discussed in [7].

The explanations considering the maxima of residual stresses in the HAZ are based on the assumption that work hardening is produced due to the developing thermal stresses. Examples of detailed calculations concerning the development of thermal respectively residual stresses (**Fig. 35**) and the development of the temperature and work hardening dependent flow stress (**Fig. 36)** as well as of the finally accumulated plastic strain confirm (**Fig. 37**) this assumption and are shown in the named figures.

Fig. 35 illustrates as an example the development of longitudinal stresses during welding of the second layer at selected times intervals and gives a first advice in which areas thermal stresses can become high enough to reach the local flow stress and produce plastic deformation and work hardening. The figure starts at 3000 s after complete cooling down from the first pass with the residual stress distribution due to the first pass. These stresses are reduced at first during the heating of the second pass, but then as a consequence of the hindered thermal expansion compressive stresses develop on both sides of the weld seam. As these stresses, magnitude for instance more than 300 MPa at 3245 s just before the temperature maximum, reach the decreasing flow stress of the heated material plastic deformation and work hardening will be the consequence in the areas close to the seam.

Very early in the cooling process (3301 s) tensile stresses grow up in the seam and in adjacent zones as a consequence of hindered thermal shrinkage and of the again increasing yield stress. During the

following intervals the tensile stresses grow obviously faster in the areas close to the weld seam than in the seam itself. It has to be assumed that in the HAZ close to the seam the work hardening produced during heating is already effective and enables higher magnitudes of stresses than in the weld seam.

During the cooling process work hardening can also occur, in the weld seam as well as again additionally in the HAZ. Therefore, after completed cooling the residual stresses in the HAZ near the fusion line can reach such appreciably high magnitudes as 380 MPa due to the work hardening influences. The shrinkage tensile stresses in the weld seam, however, remain with 275 MPa only a little bit higher than the original yield stress. As a consequence of the increasing yield stress the shrinkage of the cooling weld seam can also result in elastic strains and consequently the amount of plastic strains and therefore of work hardening is kept rather low. The very low accumulated plastic strains in the weld seam, **Fig. 37**, underline this assumption. The balancing compressive stresses in areas more remote from the seam increase at first during the cooling period and then cover a wider range with somewhat smaller magnitudes.

Adequate conclusions concerning work hardening can be drawn for the transverse stresses. They are presented for instance in [7].
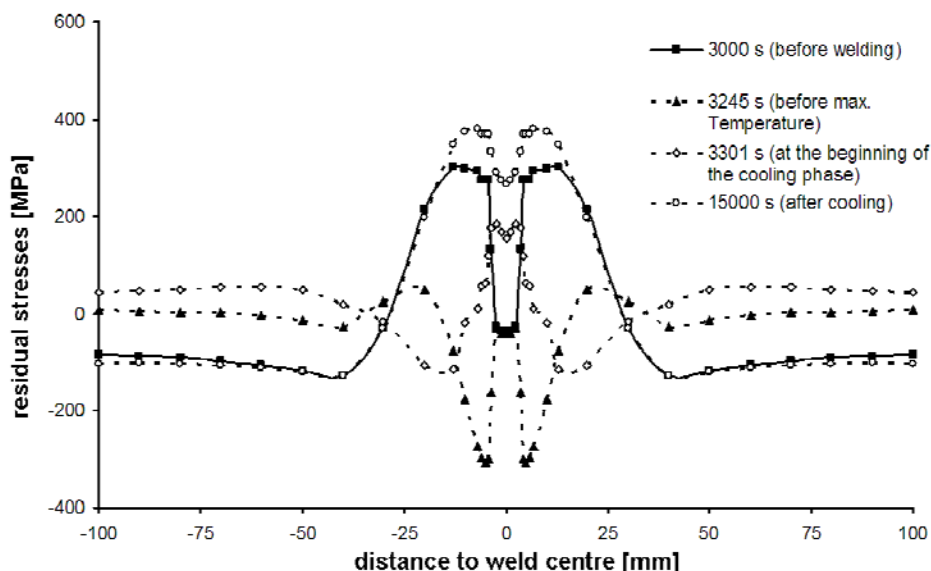

Fig. 35 Longitudinal stresses after selected time intervals during welding of the 2nd pass, 3000 s = time until complete cooling after the 1st pass [7]

The proposed strain hardening in the seam and in areas close to the seam is also confirmed in Figures illustrating the development of the temperature dependent and hardening dependent flow stress of the material (isotropic hardening). It can directly be seen at selected time intervals of the 2nd pass in **Fig. 36**. During welding of the first layer a small increase of the flow stress has already occurred due to strain hardening in areas on both sides of the seam. The beginning of the 2nd pass (3000 s) is denoted by this increased flow stress which is reduced again during the heating of the 2nd pass. At the maximum temperature the flow stress in the weld seam becomes zero (3269 s). At the beginning of the cooling period (3301 s) the flow stress has risen again and in the HAZ a small work hardening effect can already be realised. Until the end of the cooling period (15000s) the rather high flow stress value of 430 MPa is reached in the HAZ, whereas in the seam the flow stress attains a value of only 330 MPa.
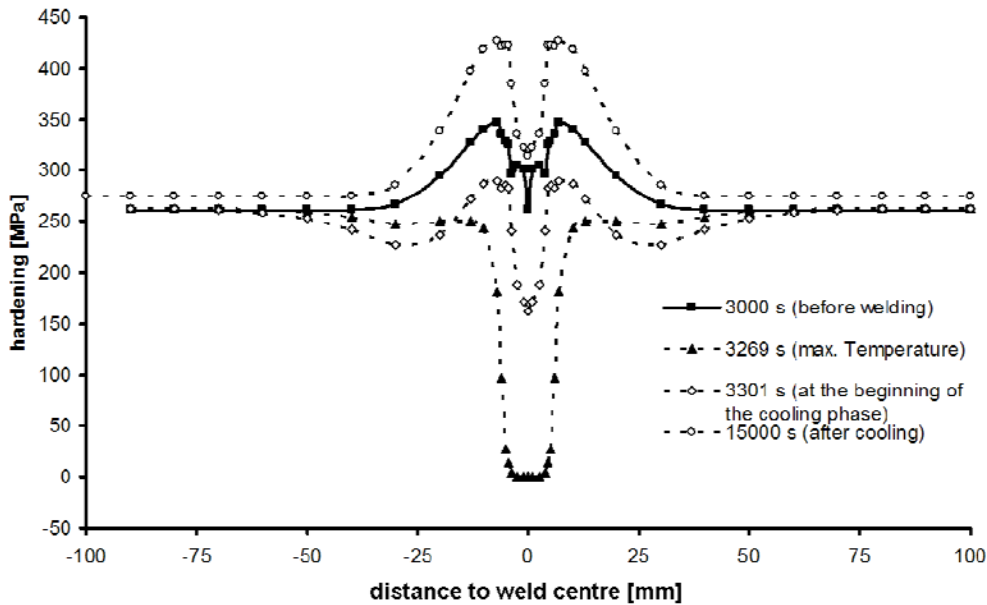
Fig. 36 Isotropic hardening variable after selected time intervals of the 2nd pass, 3000 s = time until complete cooling after the 1st pass [7]

A third indication for the work hardening effect is offered by the distribution of the calculated accumulated plastic strain in comparison with the given materials data. According to **Fig. 37** the maxima of the accumulated plastic strain are in the HAZ and represent appro**x**. 5.7 %, whereas in the weld seam only small plastic strains are revealed. A list of work hardening data for the austenitic steel given for the IIW Round Robin indicates a yield strength of 419 MPa at room temperature after a plastic deformation with a strain of 5 % [1]. Magnitudes of nearly 400 MPa of the maximum tensile stresses are obviously consistent with this yield strength value.
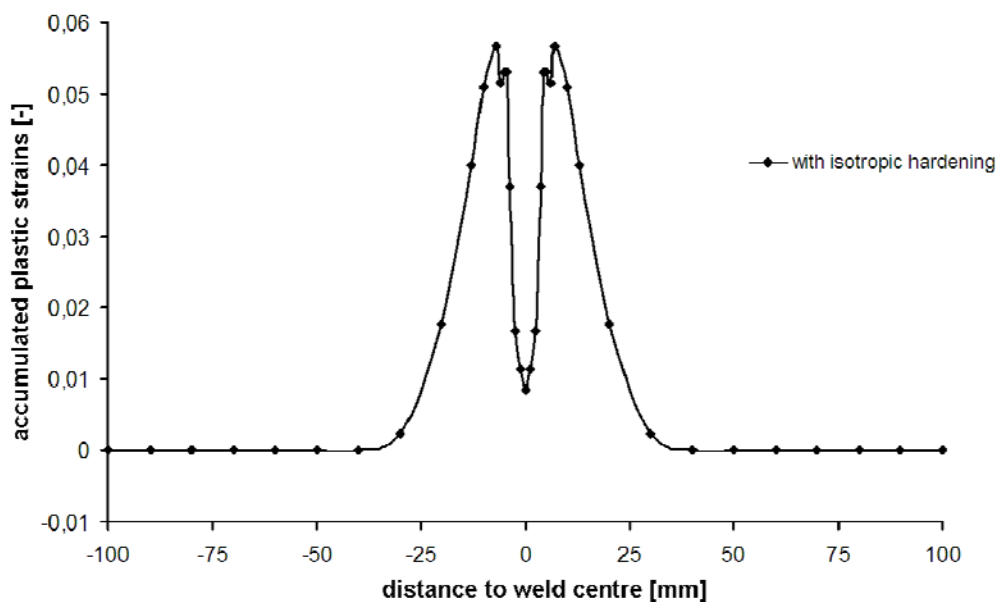

Fig. 37 Calculated accumulated plastic strains using the isotropic hardening model [7]

For an explanation of the different results of calculations with kinematic hardening respectively with isotropic hardening the possibility of an influence of the Bauschinger effect on the finally resulting

residual stresses has to be discussed. The kinematic hardening model takes into account the Bauschinger effect, whereas the isotropic model does not. Both hardening models consider the increase of compressive stresses during the heating period as a first load cycle and the opposite increase of tensile stresses during cooling as a second load cycle. But taking into consideration the Bauschinger effect with the kinematic model means that the beginning of plastic flow in the second load cycle (load reversal during cooling down) is lowered compared with the onset of plastic flow during the first load cycle (heating up). Consequently the kinematic hardening model excludes the increase of the flow stress due to work hardening in the first cycle and calculates a rather low flow stress or yield stress after completed cooling. The final tensile stresses will be limited by this relatively low yield strength. The results of calculations using the kinematic hardening law seam to indicate such a case: namely nearly constant tensile residual stresses with amounts in the range of the original yield strength at room temperature.

To take into consideration the influence of the Bauschinger effect is really necessary for cyclic plastic deformations at room or low temperatures, especially for materials with a high strain hardening exponent as for instance austenitic steels. On the other hand, indications can be found in literature [19, 20] that the Bauschinger effect is not effective – or at least not fully effective - at high working temperatures of austenitic steels. As, of course, during welding rather high temperatures exist also in the HAZ, calculations of residual stresses due to welding give more accurate results with the isotropic hardening model. It is able to account for even strong work hardening effects during the heating process and increased yield strength values can be anticipated during cooling down and finally at room temperature in the hardened HAZ close to the weld seam. Consequently the developing tensile stresses are limited only by these enhanced yield strength values and can become higher than with the kinematic hardening model. The measured and calculated maxima of the tensile residual stresses in the longitudinal direction can be understood in this way. The possible error by using the kinematic hardening model, on the other side, will be especially substantial for materials with a high hardening coefficient [7].

5.3 Discussion about hardness measurements

The considerations about the interaction of work hardening and thermal stresses respectively residual stresses discussed above seem to be quite consistent. However, HV 0.2 hardness measurements along lines transverse to the seam have shown rather constant hardness values in the seam and in the HAZ close to the seam. Higher hardness values in the HAZ close to the seam could not be observed.

This result raises the question whether or why a difference of approximately 100 MPa in the flow stress at the weld centre line and in the HAZ cannot be detected by hardness measurements. Three possible reasons can be discussed as possible explanations for this:
- work hardening occurs only in very thin surface layers, which may be penetrated by the hardness indenter with a load of 0.2 kg. An indication for this reason is the fact that X-ray stress measurements in a surface layer of app. 10 μm revealed higher tensile maxima in the HAZ than other measurements with a bigger "averaging" depth,
- the indentation by the hardness test itself may produce strong plastic deformation and work hardening in an austenitic steel and consequently a levelling of the previously existing small hardness differences,
- it is known that hardness values are somewhat lowered by tensile residual stresses. Consequently the higher tensile stresses in the HAZ may lower the measured hardness values a bit more than the lower tensile stresses in the weld seam, thus resulting in constant measured hardness values.

6. Final remarks and conclusions

6.1 Calculations of residual stresses

The "Round Robin" project with an austentic steel has shown that a rather rough estimation of the residual stress state after welding is possible without any special distinction of the hardening model to be used. But for a more precise and detailed information the chosen hardening model is of significant relevance.

Austenitic steels have a high strain hardening exponent and the thermal stresses arising during the heating and cooling of the welding process can produce considerable plastic deformation and strain hardening. It could be revealed that calculations of residual stresses due to welding show a high amount of plastic deformation. It is also known that austenitic steels show a pronounced Bauschinger effect if deformations are produced at rather low temperatures. But in the investigated case, more detailed results, which are in good agreement with measured ones, could be found by not taking the Bauschinger effect into account, i.e. the isotropic hardening model instead of the kinematic hardening model gives better results. This finding can be explained by results from literature [19, 20], indicating that in austenitic steels the Bauschinger effect is not effective – or at least less effective – if deformations are produced at higher temperatures, for instance above 300 ^{0}C. As also in the HAZ of weldments sufficiently high temperatures exist, this explanation seems to be quite reasonable for the results calculated for the considered type of an austenitic steel. But for a more general statement more detailed information about the effectiveness of the Bauschinger effect at various temperatures in welded joints of different kinds of steels would be really important.

As a result of the "Round Robin" project it can be recommended to use the isotropic hardening model – instead of the kinematic model - for calculations of residual stresses due to welding of austenitic steels. Further considerations should deal with the question whether more complex models for strain hardening, for instance the Chaboche model, could offer even better calculation results.

6.2 Experimental determination of residual stresses

For choosing an experimental method for the determination of residual stresses different aspects have to be considered, as instrumental and temporal effort, accuracy, integration volume respectively resolving capacity and of course the question whether the method is destructive or not destructive. The "Round Robin" project has evaluated special information for welded joints.

6.2.2 Non-destructive measurements

The stress analysis by means of X-rays has proven a good accuracy and the possibility of a rather high resolution concerning the stress distribution, which is important in order to detect details like local maxima or minima. The fact that by means of X-rays the stresses are detected in very thin surface layers of approximately 10 μm can be seen as advantage or as disadvantage depending on the aim of the investigation.

In the "Round Robin" investigations, the method has indicated the highest stress maxima in the detected thin layers of the HAZ. In the base material far away from the weld seam the special feature of the method became obvious, that grinding stresses, superimposing the welding stresses in thin layers, may be detected. The method has not been used to detect stress gradients in the "Round Robin" tests. This would be possible in steps with very thin layers, but it would be very time

consuming. The big grain size often found in weld seams resulted in problems, which have been solved with a more specialized equipment.

Methods using synchrotron radiation have not been examined in the "Round Robin" tests, but could be rather promising.

With the method of neutron diffraction the measured stresses are integrated over thicker layers, e.g. 3 mm, compared to the X-ray method. This can provide more evidence of the residual stresses due to welding, as disturbing surface effects are at least minimized in the result. Such a result was obvious in the "Round Robin" test. The measurements by means of neutron diffraction offered a clear description of the residual stress state with tensile and compensating compressive stresses over a wide range. A big advantage of this method is of course the possibility to detect stresses in deeper layers of thick welded plates, as proved in the "Round Robin" tests for instance in a depth of 15 mm, and to get information about the stress gradient down to such a depth below surface. The instrumental effort of this method is of course very big.

6.2.3 Semi-destructive measurements

As semi-destructive measurements various types of the hole drilling methods are commonly used for stress evaluations in welded joints. The advantage of the conventional method is a rather small instrumental and temporal effort.

In the "Round Robin" investigations a very specific method using electronic Speckle-interferometry for the measurement of deformations after hole drilling was incorporated. This method provided obviously accurate stress distributions versus distance from the weld centre line averaging the residual stresses over the drilling depth of 1 mm. The result is in very good agreement with calculations of residual stresses using the isotropic hardening model. The method has the advantage to offer interesting additional information about the stress state and the principal stresses.

The results of the conventional incremental hole drilling method in the "Round Robin" tests indicated a rather good agreement with other measurements of the surface stress minima at the weld centre line and the maxima in the HAZ. But the results of longitudinal residual stresses versus depth below surface at the weld centre line described by various laboratories show obviously strong inconsistencies, whereas the courses of residual stresses versus depth below surface at the positions of the stress maxima are mainly consistent with the same tendencies. The differences between some surface stress values could be attributed to the polishing or grinding, which was necessary at the locations of measurements, but it is not sure whether the inconsistencies in the stress gradients below the weld centre line could also be explained with an influence of grinding on the stresses in surface layers.

The "Round Robin" tests indicated clearly that with some experience measurements with hole drilling methods offer the possibility of good estimations of the residual stress state after welding with a minimum effort.

7. References

[1]   JANOSCH J.J.: IIW Round Robin Protocol for Residual Stress and Distortion Prediction, Phase II (Proposal Rev. 1)", *IIW-Document IIW-X/XV-RSDP-59-00*

[2]   JANOSCH, J.J.; *IIW-Documents IIW-X/XV-RSDP-60-01, IIW-X/XIII/XV-RSDP-68-02, XV-1121-02, XIII-1904-02*, IIW-X/XV-RSDP-68-03, *IIW "Round Robin" Update Results for Residual Stress and Distortion Prediction IIW-X/XIII/XV-RSDP-97-04*

[3]   JANOSCH, J.J.: IIW "Round Robin" Protocol for 3-Dimensinal Welding Residual Stress and Distortion Prediction, *IIW-Document X/XIII/IV-RSDP-75-03*

[4]   RADAJ, D.: Heat Effects of Welding - Temperature Field, Residual Stress, Distortion *Springer-Verlag, Berlin,* 1992

[5]   BRAND, M., SIEGELE, D.: State of the Numerical Round Robin Residual Stress Results, *IIW-Document X-1648-08*

[6]   GOLDAK, J.; Charkravarti, A. & Bibby, M.: A new finite element model for welding heat sources *Metallurgical and Materials Transactions B,* 1984, *VOLUME 15*, pp. 299-305

[7]   LOOSE, T., SAKKIETTIBUTRA, J., WOHLFAHRT, H.: New 3D-calculations of residual stresses consistent with measured results of the IIW Round Robin Programme. *Mathematical Modelling of Weld Phenomena 9, pp. 369-390, Verlag der technischen Universität Graz, Graz,* 2010

[8]   WOHLFAHRT, H: Report on the Experimental Round Robin Tests on Residual Stresses 2005, *IIW-Document X/XIII/XV- RSDP-112-05*

[9]   JANOSCH, J.J.: „Round Robin phase II – 3D modelling. Updated results", *IIW Document II-X/XIII/XV-RSDP-114-05.*

[10] JANOSCH, J.J.: "International Institute of Welding work on residual stress and its application to industry", *International Journal of Pressure Vessel and Piping*, *Vol. 85*, 2008, pp. 183-190.

[11] WOHLFAHRT, H.: New calculations checking an adequate materials law. New results on distortion measurements. Report on the Round Robin Tests on Residual Stresses 2009. *IIW Document IIW- X-1668-09, IIW-XIII-2291-09, IIW-XV-1326-09.*

[12] WOHLFAHRT, H.: Reports on the Experimental Round Robin Tests on Residual Stresses, Joint Working Group of Commission X/XIII/XV *IIWDocument-XIII-2144-06 / XV-1227-06 / IIW-RSDP-X/XIII/XV-115-06, IIW-Document IIW- X-1633-07, IIW-XIII-2199-07, IIW-XV-1263- 07*

[13] WOHLFAHRT, H., DILGER, K.: New results of the IIW Round Robin Residual Stress Measurements. Report on the Experimental Round Robin Tests on Residual Stresses 2008. *IIW- Document IIW-XIII-2241-08, IIW-XV-1283-08*

[14] LOBANOV, L.M: Report from E.O. Paton Electric Welding Institute, Kiev, for *IIW Report IIW-XIII-2241r-08, IIW-XV-1283r-08*, 2008.

[15] LOBANOV, L.M., PIVTORAK, V.A., SAVITSKY, V.V., TRACHUK, G.I.: Procedure for Determination of Residual Stresses in Welded Joints and Structural Elements Using Electron Speckle-Interferometry, *The Paton Welding Journal, 1/2006, pp. 24-29.*

[16] INSTITUTE FOR JOINING AND WELDING, UNIVERSITY OF BRAUNSCHWEIG: ADDITIONAL MEASUREMENTS

[17] GEORG, H., BENEDIKT, H.: Indications on Formation and Effect of Delta-Ferrite in Austenitic Alloys (Material No. 1.4404 / 1.4435), in German, Henkel-Epol, *2003, Aufsatz Nr. 32 / Rev. 00*

[18] BRAND, M.: Further Development of Methods of Numerical Welding Simulation, PhD-Thesis, in progress, (in German)

[19] MANNINEN, T., MYLLYKOSKI, P., TAULAVUORI, T., KORHONEN, A.S.: Large-strain Bauschinger effect in austenitic stainless steel sheet, *Materials Science and Engineering* A 499 (2009) pp. 333-336

[20] MATAYA M.C. AND CARR M.J.: The Bauschinger Effect in a Nitrogen-strengthened Austenitic Stainless Steel, *Materials Science and Engineering, 57 / 2 (1983) pp. 205-222.*

8. Acknowledgement